

THE EXPERIMENTAL AND THEORETICAL INVESTIGATIONS OF WINDMILLS

Iwasaki, Matsunosuke
Research Institute for Applied Mechanics, Kyushu University

<https://hdl.handle.net/2324/7157918>

出版情報 : Reports of Research Institute for Applied Mechanics. 2 (8), pp.181-229, 1953-12. 九州大学応用力学研究所
バージョン :
権利関係 :

THE EXPERIMENTAL AND THEORETICAL INVESTIGATIONS OF WINDMILLS

By Matsunosuke IWASAKI

Summary

The experimental data, which can be the object of the comparison with the theory, and in which the data of the drag coefficients of the windmills are contained, are obtained for the 2, 3, 4 and 6 bladed windmills. The simple formulas for the calculation of the coefficients of torque, drag and power of windmills are found, and these formulas agree well with the results of the experiments. The distributions of the lift coefficients along the blades are calculated by these formulas at the maximum power states. The performances of the windmills having the circular cylinder outside of them are investigated by the experiments and analyses.

1. Introduction. The momentum theory of windmills was established by Glauert,¹⁾ while the experimental data of windmills can be found in the reports of the results of wind-tunnel tests at Göttingen,²⁾ Sabinin's work³⁾ and Sanuki's paper.⁴⁾ Though Glauert's theory is very instructive to know some characteristics of windmills qualitatively, it is not suitable for estimating the performances of windmills quantitatively. The experiments at Göttingen are restricted only to the practical windmills, so that these data cannot be the object of the comparison with the theory of windmills. The Sabinin's experiment is restricted to a special case of windmill blown by the side wind. Sanuki's experiment is the more systematized and complete one than the others, but the effect by the boss of windmills are not eliminated, and his paper contains no data of the drag coefficients of windmills.

As mentioned above, there are small numbers of the experiments and theories of windmills, and they are not appropriate to the quantitative and precise investigation of windmills. Of course it is not necessary to investigate the performances of windmills too precisely, because windmills are not used in so exact conditions. But, from the theoretical standpoint, it

¹⁾ Durand: *Aerodynamic Theory*, Vol. IV, Chap. XI, pp. 324-332, 1935.

²⁾ *Ergebnisse der Aerodynamischen Versuchsanstalt zu Göttingen*, III. Lief., pp. 139-144, and IV Lief., pp. 118-123.

³⁾ Wien-Harms: *Handbuch der Experimentalphysik*, IV 3. Teil, p. 408, 1931.

⁴⁾ M. Sanuki: *Studies on Biplane Wind Vanes, Ventilator Tubes and Cup Anemometers* (I), *Papers in Meteorology and Geophysics*, Vol. I, No. 2-4, pp. 279-290, Dec. 1950.

may have some meaning to make a precise experiment with which the comparison of the theoretical results is possible, and to find such simple theoretical formulas for the calculation of the torque, power and drag of windmills that agree well with the results of experiments. So the author has carried out the experiments and some theoretical analyses from the latter viewpoint.

The remarkable increase in the power of windmills by ventilator tubes is found in the Sanuki's experiments. This increase seems to be resulted from the two effects: the first one is the acceleration of wind velocity by the ventilator tube, and the second the prevention of the flow around the tips of blades by it. To estimate the gain by the latter effect the performances of wind-mills with rings were measured, while some analyses were made. By the experimental and theoretical investigations, we found that the gain by this effect was very smaller than the one due to the acceleration of wind velocity.

The experiment of the windmills with rings was performed by Tanaka⁵⁾ at the author's laboratory. Moreover he made the preparatory theoretical investigation about them. The author should like to appreciate his contribution to this subject.

2. The Instruments and Methods of Experiments. The wind tunnel used in the experiment has the elliptic cross section of $1.5\text{ m} \times 2.5\text{ m}$.⁶⁾ The minimum and maximum speeds of the tunnel are 1.5 m/sec and 28 m/sec respectively. The data of the blades of the windmills used in the experiment are shown in Table 1. The sections of blade elements are normal to the straight line which connects the centers of gravity of all sections together, so that the blade are shaved by using straight plane gauges.

The data of the airfoil shown in this Table is the one measured at Göttingen, because the exact correction factors for the wall interference of the wind tunnel is not yet determined in the author's wind tunnel.

The blades are made of mahogany and their roots are inserted in the cylinders of duralumin.

Being polished with sand paper before and after each spraying, the surfaces of blades are sprayed with the transparent lacquer three times or more. The blades are attached to the boss of oak. The two, three, four and six bladed windmills were used in the experiment.

The dynamometer is shown in Figure 2. This dynamometer is designed so that the measurement of the torque which is absorbed by the tachometer-dynamo and the friction of bearings may be possible by means of the second torque bar 4. The main shaft is supported by the two self-aligning ball bearings at the both ends. With these bearings the dynamometer is

⁵⁾ Y. Tanaka: On the tip loss of windmills, (the First Report) (in Japanes), Memoirs of the Junior College of Kagoshima Prefecture, Japan. No. 3, 1952, pp. 1-11.

⁶⁾ M. Iwasaki: On the Elliptic $2.5\text{ m} \times 1.5\text{ m}$ Wind Tunnel of Kyushu University (the First Report) (in Japanes), Technology Reports of the Kyushu University, Vol. 25, Nos. 3-4, March 1953, pp. 114-118.

TABLE 1. The data of the blade and the airfoil section.

r/R	c/R	β ($\beta_{0.75R} = 40^\circ$)	α	C_L	C_D
0.34	0.307	$59^\circ 28'$	-7.17°	-0.195	0.255
0.40	0.308	$55^\circ 40'$	-5.81°	-0.045	0.0147
0.60	0.314	$45^\circ 31'$	-4.39°	0.092	0.0119
0.75	0.326	$40^\circ 00'$	-2.98°	0.231	0.0106
0.85	0.340	$37^\circ 07'$	-1.55°	0.366	0.0106
0.925	0.355	$35^\circ 16'$	-0.14°	0.505	0.0122
0.975	0.368	$34^\circ 11'$	1.25°	0.648	0.0139
1.000	0.378	$33^\circ 42'$	2.68°	0.782	0.0155
			4.10°	0.919	0.0181
			5.57°	1.045	0.0224
			7.12°	1.151	0.0281
			8.74°	1.240	0.0374
			10.60°	1.273	0.0573

R : radius of windmill = 0.5m.

B : blade number = 2, 3, 4 and 6.

The outer diameter of the boss = 0.27 m.

Airfoil section: Göttingen 623

(zero lift angle = -5.21° , measured from the bottom straight line.)

α : geometrical angle of attack measured from the bottom straight line.

Aspect ratio = ∞

$Re = 4.1 \times 10^5$

(from *Ergeb. Aerody. Versuch. Göttingen IV Lief. S. 57.*)

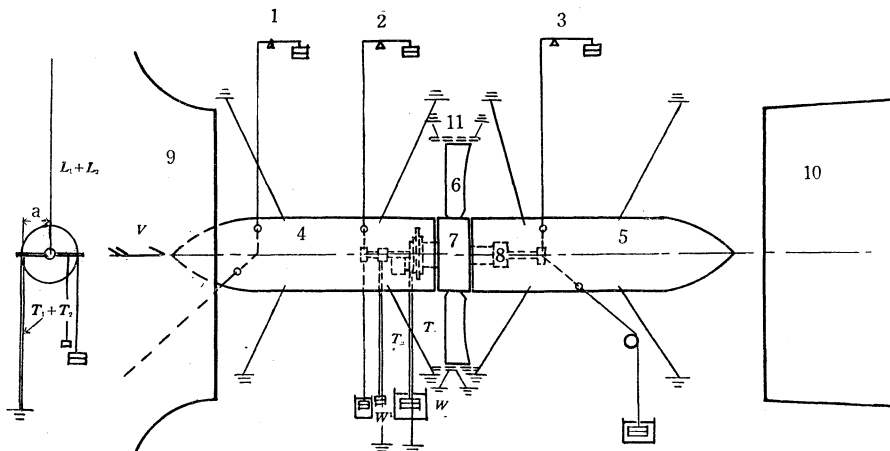


FIG. 1. Apparatuses for the experiments

- | | |
|---|--|
| 1. drag balance. | 11. circular cylinder (inner dia. $\div 1.020$ m, length = 0.3 m). |
| 2. the first lift balance. | a. effective radius of pulley. |
| 3. the second lift balance. | L_1, L_2 . indicated values of the first and second lift balances. |
| 4, 5. covers of semi-monocoque structure. | T_1, T_2 . torque loads. |
| 6. blades of windmill. | V . wind velocity. |
| 7. boss. | W . torque weight. |
| 8. dynamometer. | W_1 . auxiliary torque weight. |
| 9. jet of wind tunnel. | |
| 10. intake of wind tunnel. | |

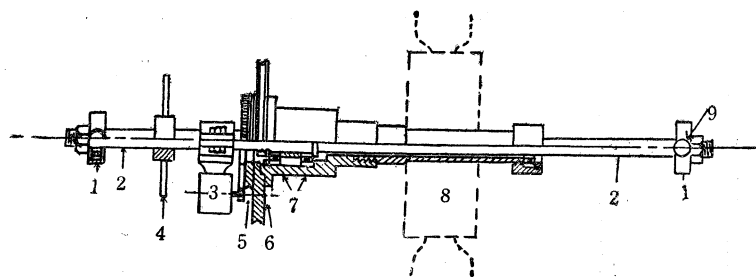


FIG. 2. Dynamometer for windmills

- | | |
|--|----------------------------------|
| 1. self-aligning ball-bearings. | 7. main bearings. |
| 2. main shaft. | 8. windmill. |
| 3. tachometer dynamo. | 9. small ball-bearings which are |
| 4. auxiliary torque bar. | used to hang the dynamometer |
| 5, 6. pulleys small and large. diameters | to the balances. |
| are about 0.12 m and 0.20 m. | |

hanged to the first and the second lift balances of the ordinary wind tunnel balances (see Figure 1). The large and small pulleys 5 and 6 in Figure 2 are used to brake the windmills. The belt used to brake the pulleys is a leather belt of a ordinary sewing machine. The tensions of wires T_1 and T_2 (see Figure 1) are measured by the balances. The torques absorbed in the bearings and the tachometer-dynamo are included in these measured values, because these torques is transmitted to the balances as the reaction of the tensile forces of the wires $T_1 + T_2$. In using this instrument, it may happen that the side force of the windmill enters into the measured torque. To testify this we measured the torque directly in aid of the spring balance which was attached to the end of the wire T_1 . The results obtained by this method was compared with the values obtained by the balance of the wind-tunnel, and it was found that they agreed within the error of experiment, so that the method by the wind tunnel balances was adopted throughout the experiment. The dynamometer is connected to the drag balance so that the drag may be measured simultaneously. The dynamometer is shielded from the wind by the cover of semi-monocoque structure which is attached to the wind tunnel wall and seperated from the dynamometer. With this cover the flow in front of the windmimills becomes parallel to the axis of the wind tunnel, so that the effect of the boss on the windmill is reduced. This method is according to the experiment of propellers by Lock, Bateman and Nixon.⁷⁾

The effective radius of the pulley a (in Figure 1.) is determined by a known moment applied to the dynamometer statically, and this caliblation was repeated often during the experiment. In the dynamical state, a thus determined may show somewhat different value from the statical one, but we neglected the error due to this difference.

⁷⁾ C. N. H. Lock, H. Bateman and H. L. Nixon: Wind Tunnel Tests of High Pitch Aircsrew (Part I), Reports and Memoranda No. 1673, 1935-36, pp. 195-223.

The boss drag is subtracted from the values measured in the experiment of windmills. The boss drag is obtained in the state in which the blades are detached and the holes of blade-roots are filled with wood, so that the drag of the boss thus measured does not contain the pressure drag which arises from the difference of pressure in front and back of the windmill. Because the boss drag which should be subtracted from the value of the measured drag of windmills is small, the drag coefficients of windmills shown in the latter figures will show somewhat larger value than the true ones.

The number of revolution of the windmills is measured with the electric tachometer which is calibrated by using the electro-magnetic oscillograph and the 100 cycles tuning-fork.

The wind velocity is calculated from the pressure which is taken from the wall of the wind tunnel at the root of the jet. The pressure is calibrated against the pitot-static tube which is surveyed through the plane of the windmill when the windmill is detached. The deviation of the correction factor from the ones of the local points is within ± 2 per cent.

The angle of blades is measured at the 75 per cent of the radius of the windmills and it is the angle between the windmill plane and the bottom flat surface of airfoil at the radius. The angles of blades are changed from 10° to 80° with the interval of 10° .

3. The Results and Discussions. One example of results of experiments is shown in Figure 3. The scattering of the points of experiments are nearly within the order of this example. The results are plotted in Figures 4 - 15, and tabulated in Table 2. These curves are the smoothed curves.

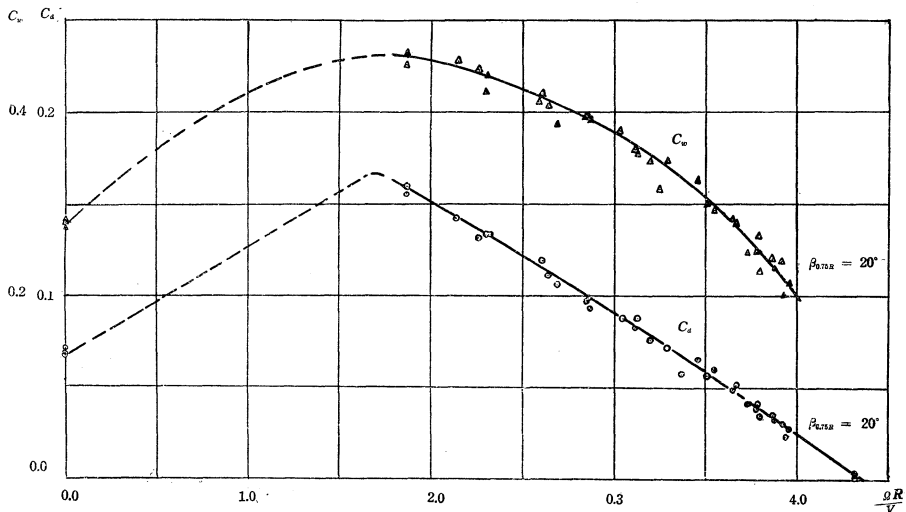


FIG. 3. The example of results of experiments
(C_d and C_w for the three bladed windmill).

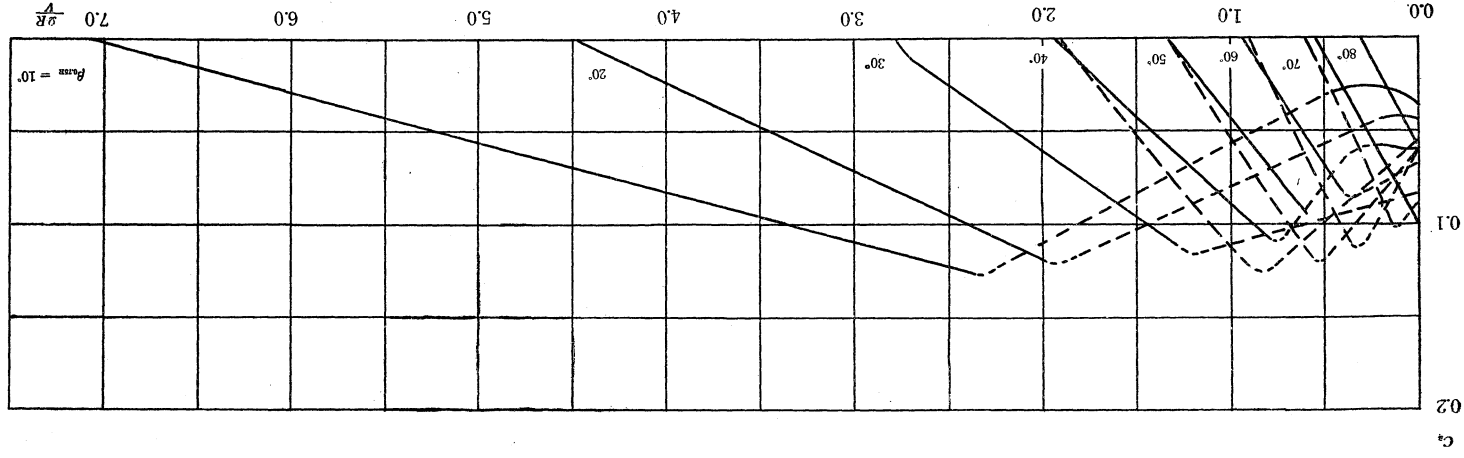
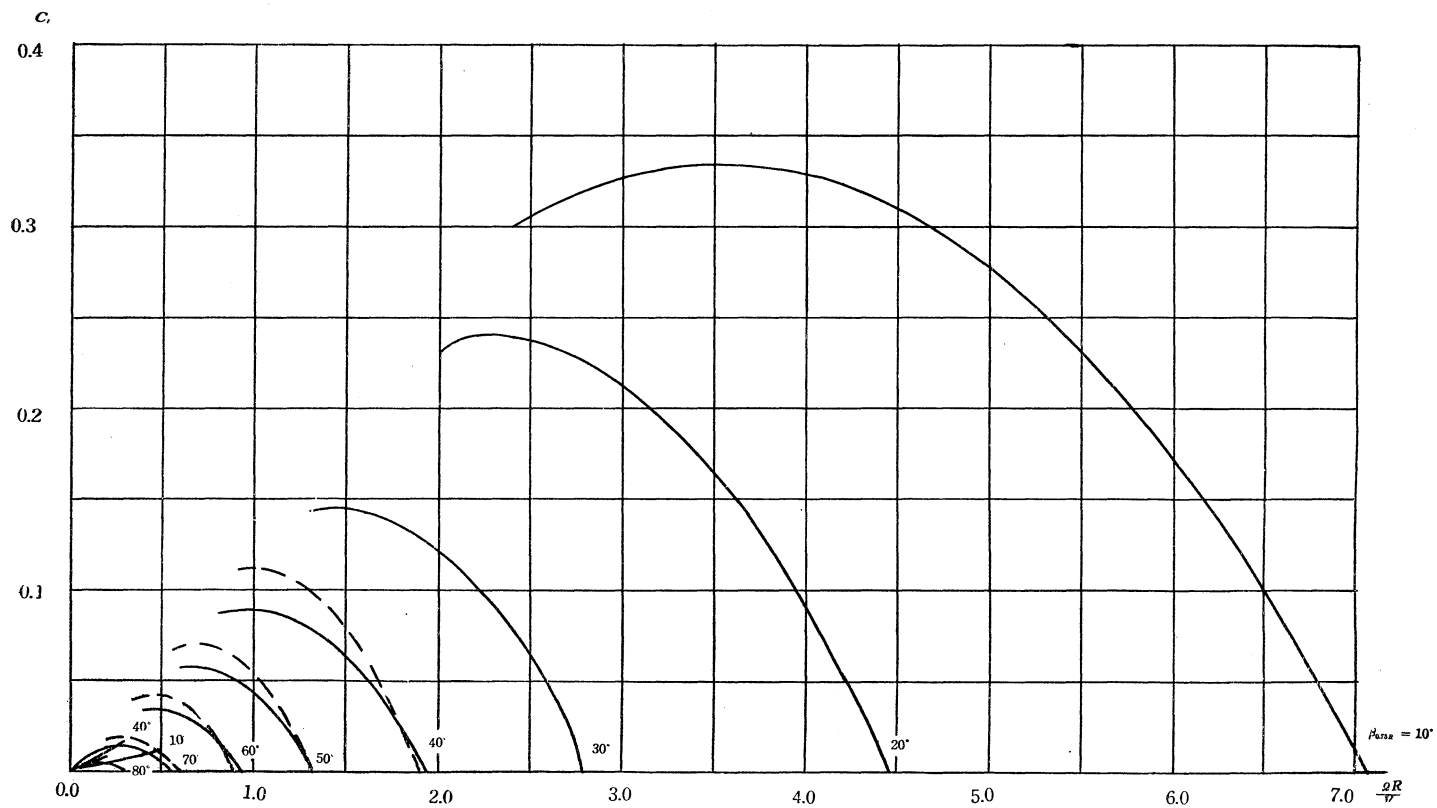


Fig. 4. The C_d curves for the two bladed windmills.

FIG. 5. The C_l curves for the two bladed windmills.

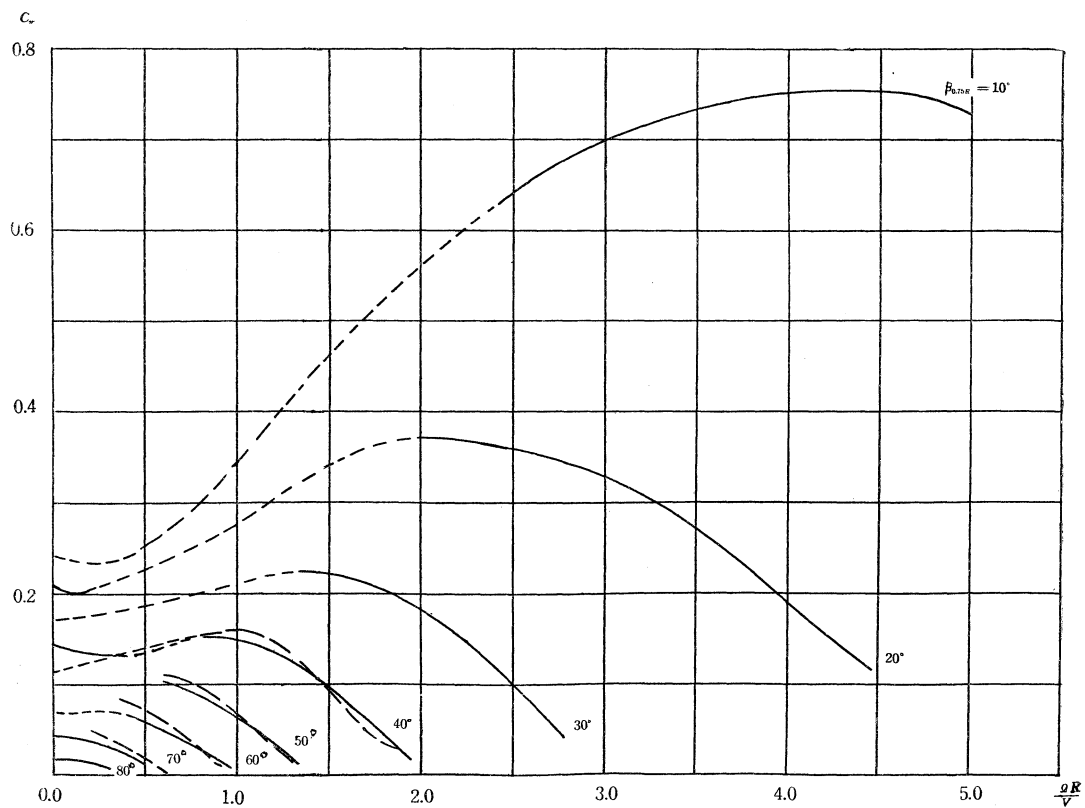
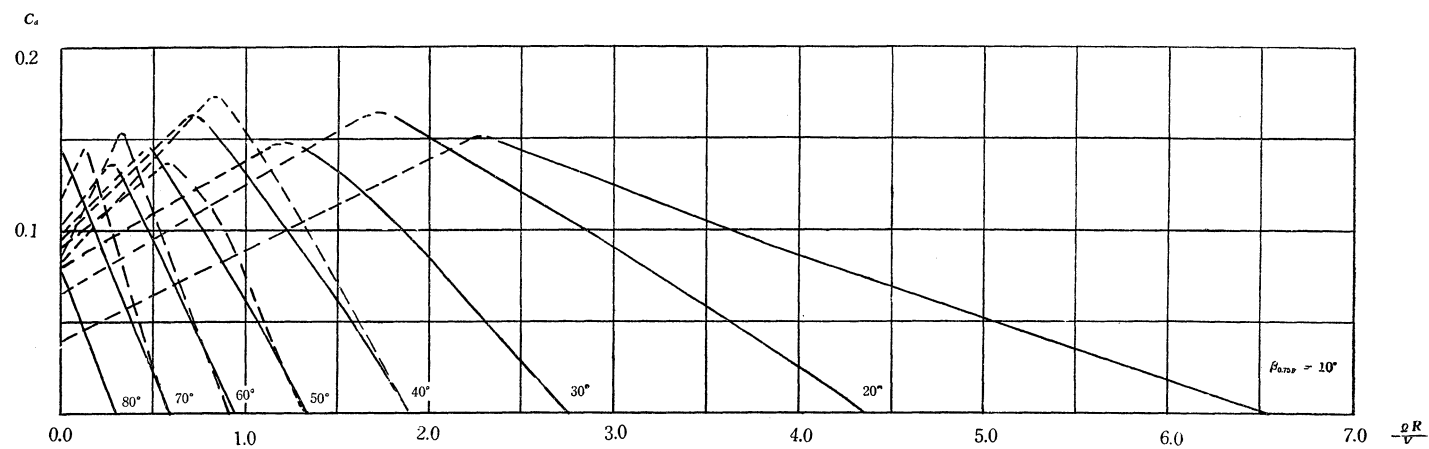
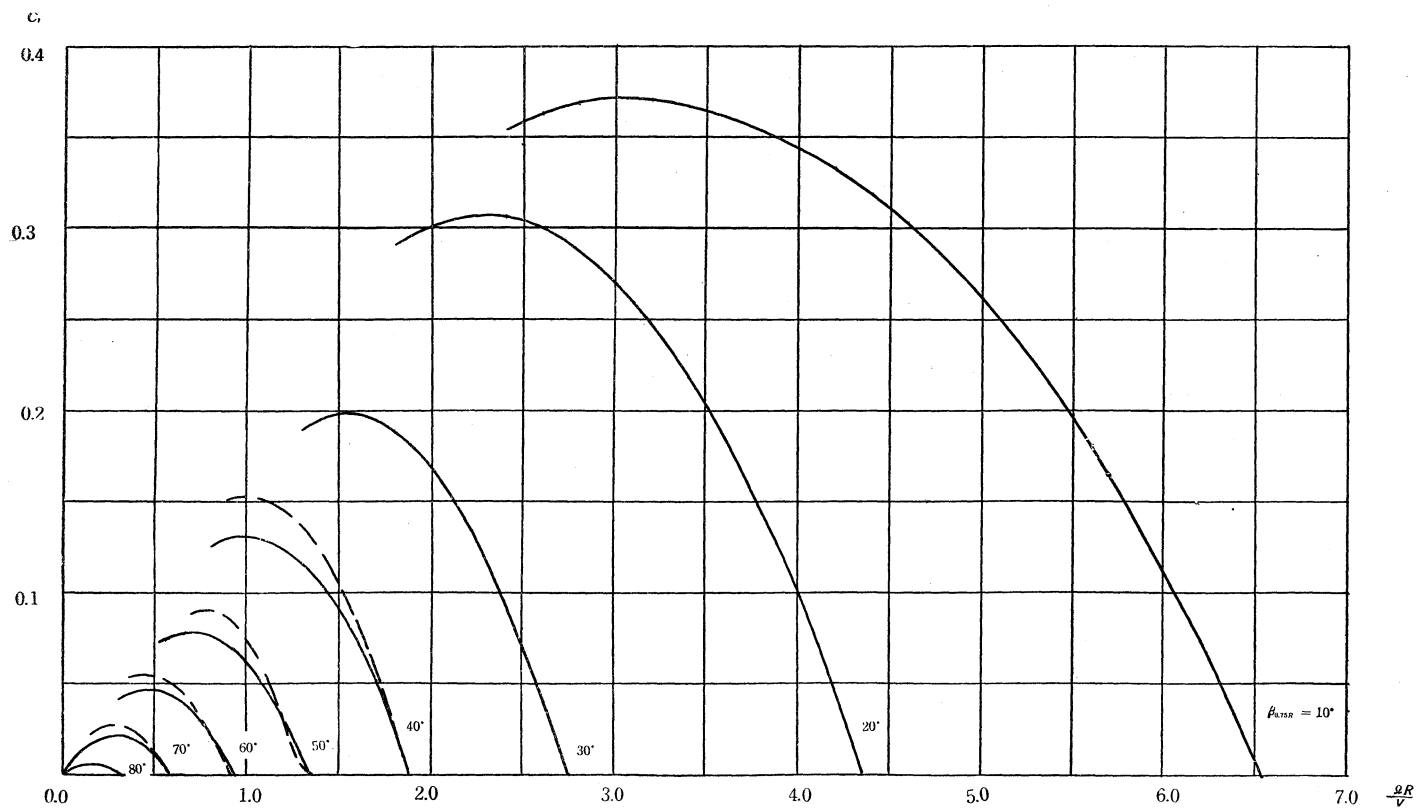
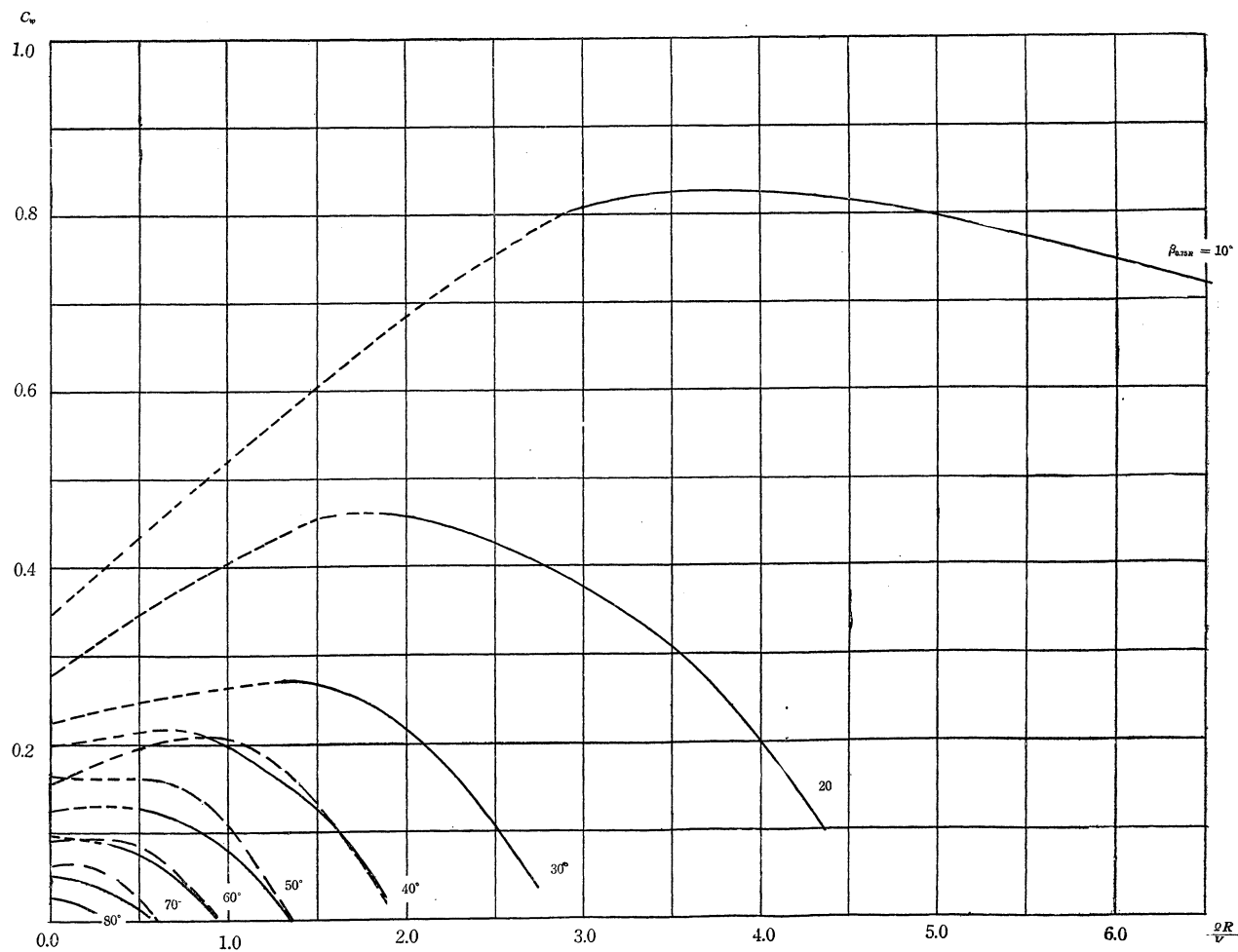


FIG. 6. The C_w curves for the two bladed windmills.

FIG. 7. The C_d curves for the three bladed windmills.

FIG. 8. The C_l curves for the three bladed windmills.

FIG. 9. The C_w curves for the three bladed windmills.

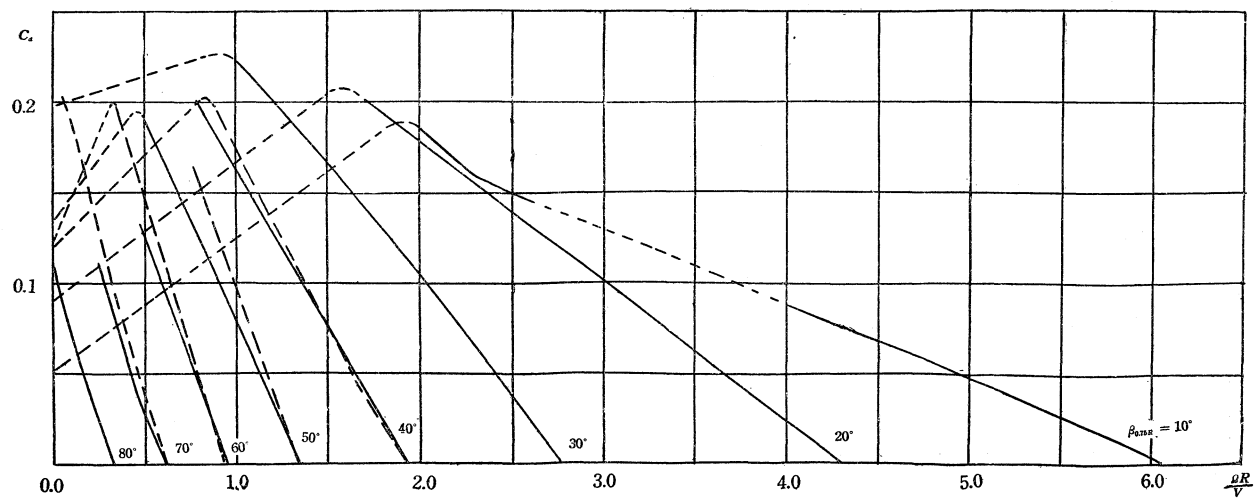
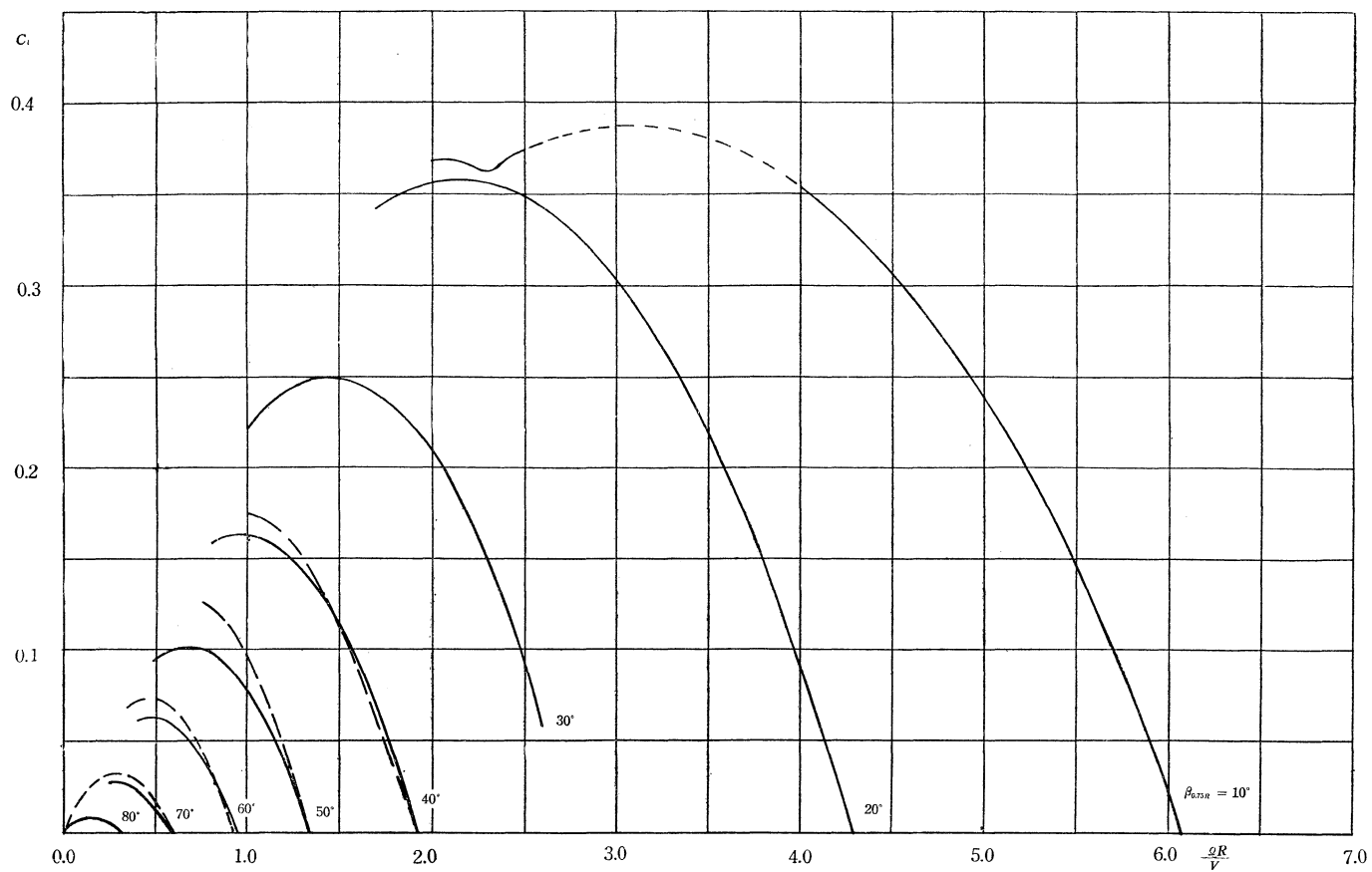
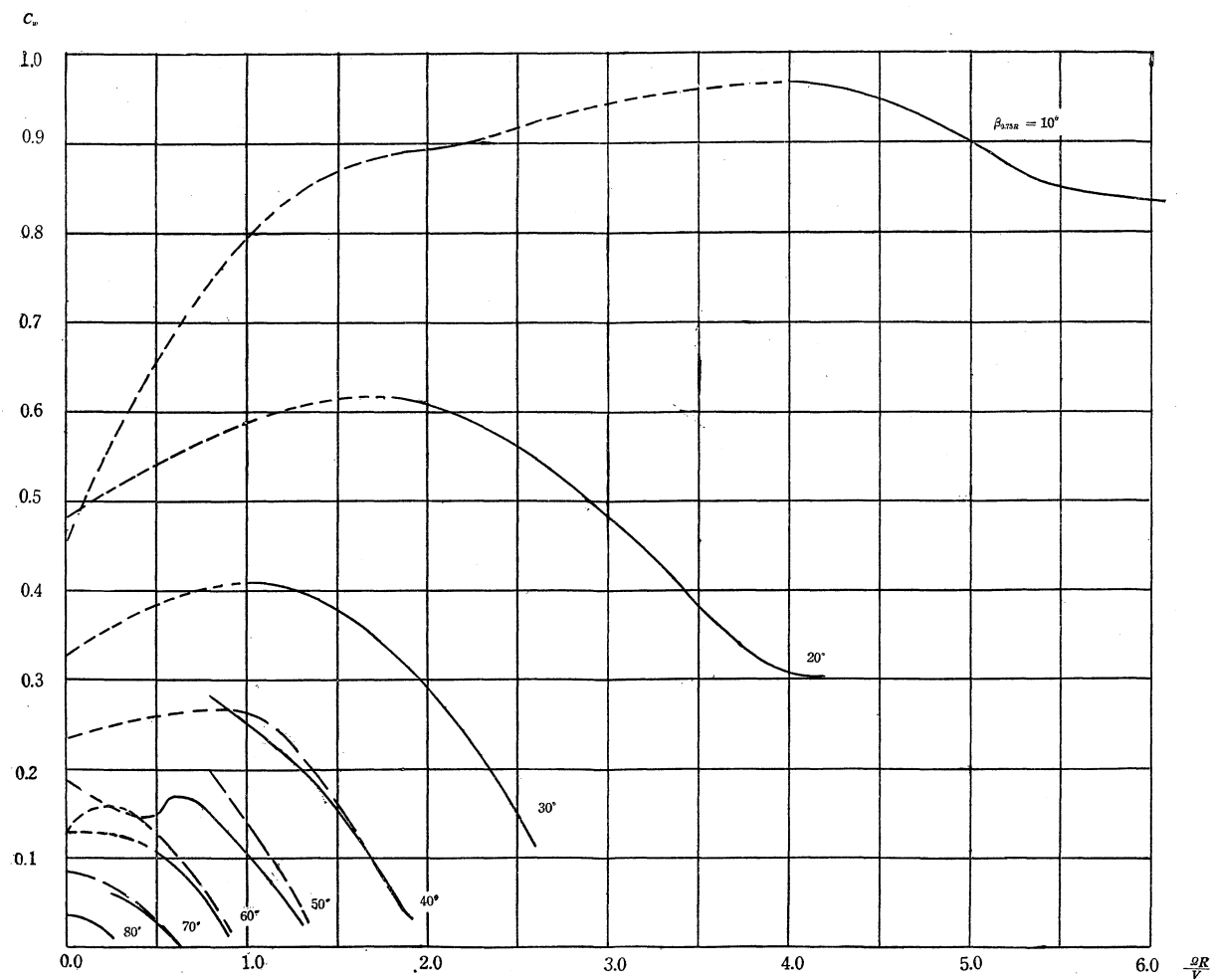
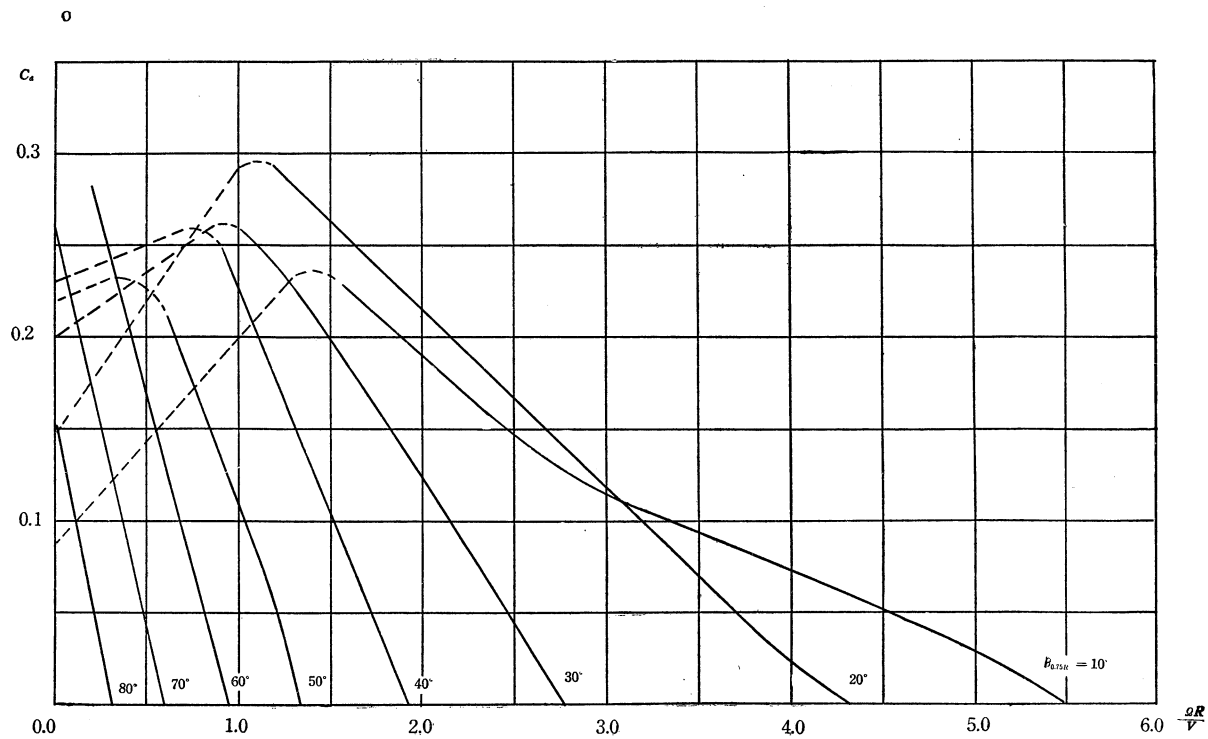
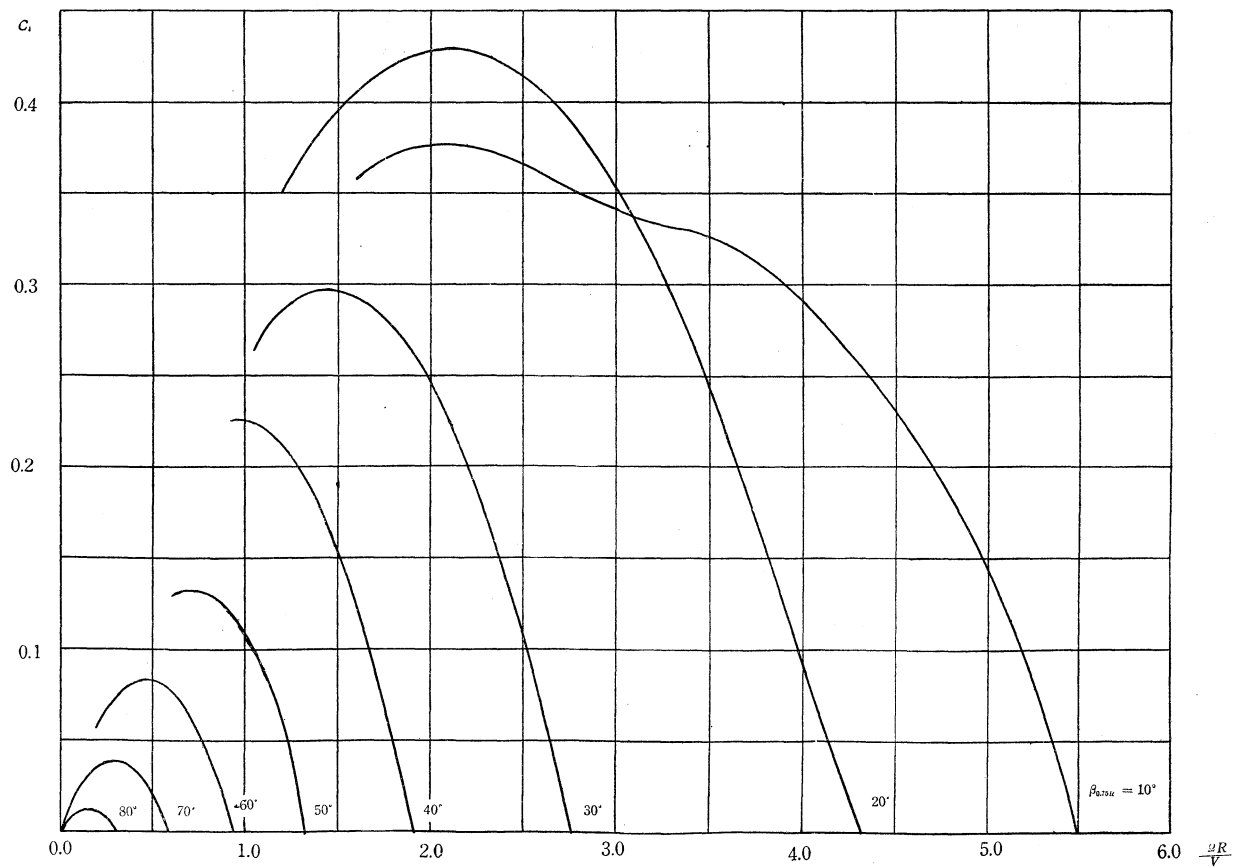


FIG. 1C. The C_d curves for the four bladed windmills.

FIG. 11. The C_l curves for the four bladed windmills.

FIG. 12. The C_w curves for the four bladed windmills.

FIG. 13. The C_d curves for the six bladed windmills.

FIG. 14. The C_T curves for the six bladed windmills.

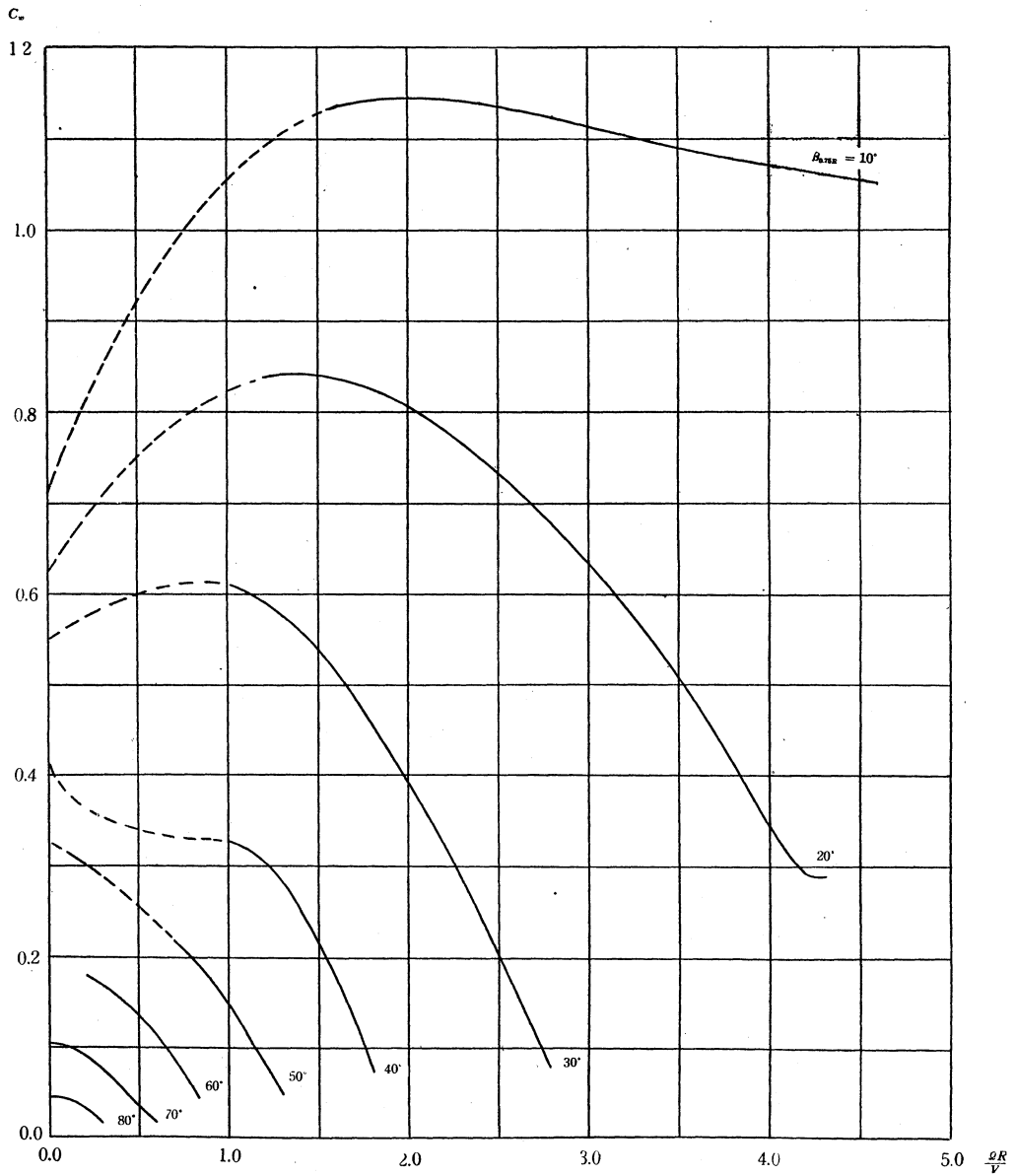
FIG. 15. The C_w curves for the six bladed windmills.

TABLE 2. The Values of C_d , C_l and C_w
read from the smoothed curves.

(The values of $\beta_{0.75R}$ are measured from the bottom flat surface of the airfoils.)

$\Omega R/V$	C_d	C_l	C_w
0.00	0.0365	0	0.241
0.10	0.0300	0.0030	0.236
0.20	0.0263	0.0053	0.234
0.30	0.0255	0.0077	0.235
0.40	0.0263	0.0105	0.240
0.45	0.0275	0.0124	0.245
2.40	0.125	0.300	0.626
2.60	0.120	0.312	0.656
2.80	0.114	0.319	0.681
3.00	0.109	0.327	0.700
3.20	0.104	0.333	0.715
3.40	0.0982*	0.334	0.728
3.60	0.0928	0.334	0.738
3.80	0.0875	0.333	0.747
4.00	0.0820	0.328	0.753
4.20	0.0768	0.323	0.755
4.40	0.0715	0.315	0.755
4.60	0.0661	0.304	0.752
4.80	0.0608	0.292	0.743
5.00	0.0555	0.278	0.724
5.50	0.0422	0.232	
6.00	0.0286	0.172	
6.50	0.0153	0.0995	
7.07	0	0	

$B = 2$
 $\beta_{0.75R} = 10^\circ$

$\Omega R/V$	C_d	C_l	C_w
0.00	0.044	0	0.207
0.10	0.042	0.0042	0.200
0.20	0.043	0.0086	0.204
2.00	0.119	0.238	0.371
2.20	0.109	0.240	0.368
2.40	0.0996	0.239	0.362
2.60	0.0900	0.234	0.353
2.80	0.0804	0.225	0.342
3.00	0.0707	0.212	0.328
3.20	0.0611	0.196	0.308
3.40	0.0515	0.175	0.286
3.60	0.0427	0.154	0.255
3.80	0.0325	0.124	0.225
4.00	0.0224	0.0896	0.190
4.20	0.0133	0.0559	0.157
4.40	0.0040	0.0176	0.128
4.46	0	0	0.115

$B = 2$
 $\beta_{0.75R} = 20^\circ$

$\Omega R/V$	C_d	C_l	C_w
0.00	0.0835	0	0.172
1.3	0.110	0.143	0.224
1.4	0.103	0.144	0.223
1.5	0.0962	0.144	0.221
1.7	0.0819	0.139	0.211
1.9	0.0678	0.129	0.195
2.1	0.0537	0.113	0.170
2.3	0.0396	0.0911	0.137
2.5	0.0255	0.0638	0.100
2.7	0.0100	0.0270	0.061
2.78	0	0	0.044

$B = 2$
 $\beta_{0.75R} = 30^\circ$

$\Omega R/V$	C_d	C_l	C_w
0.00	0.0612	0	0.142
0.1	0.0592	0.0059	0.138
0.2	0.0576	0.0115	0.135
0.3	0.0568	0.0170	0.133
0.8	0.108	0.0864	0.154
1.0	0.0889	0.0889	0.148
1.2	0.0703	0.0844	0.137
1.4	0.0516	0.0722	0.112
1.6	0.0328	0.0525	0.0795
1.8	0.0134	0.0241	0.0435
1.945	0	0	0.0170

$B = 2$
 $\beta_{0.75R} = 40^\circ$

$\Omega R/V$	C_d	C_l	C_w
0.6	0.0950	0.0570	0.104
0.7	0.0820	0.0574	0.0964
0.8	0.0690	0.0552	0.0865
0.9	0.0564	0.0508	0.0757
1.0	0.0434	0.0434	0.0643
1.1	0.0306	0.0337	0.0505
1.2	0.0174	0.0209	0.0350
1.3	0.0046	0.00598	0.0177
1.34	0	0	0.0119

$B = 2$
 $\beta_{0.75R} = 50^\circ$

* This fourth figure 2 is not necessary in this column, but it is convenient to write the three significant figures for the calculation of the values of C_l and C_d which have the same accuracy according to the relation $C_l = \Omega R/V C_d$ and besides the curves

TABLE 2 (cont'd)

$\Omega R/V$	C_d	C_l	C_w
0.00	0.0675	0	0.0675
0.40	0.0835	0.0334	0.0666
0.50	0.0680	0.0340	0.0588
0.60	0.0525	0.0315	0.0490
0.70	0.0373	0.0261	0.0386
0.80	0.0220	0.0176	0.0270
0.945	0	0	0.0110
$B = 2$ $\beta_{0.75R} = 60^\circ$			
$\Omega R/V$	C_d	C_l	C_w
0.00	0.101	0	0.0422
0.10	0.0825	0.0083	0.0403
0.20	0.0645	0.0129	0.0364
0.30	0.0463	0.0139	0.0303
0.40	0.0283	0.0113	0.0225
0.50	0.0100	0.0050	0.0120
0.555	0	0	
$B = 2$ $\beta_{0.75R} = 70^\circ$			
$\Omega R/V$	C_d	C_l	C_w
0.00	0.0580	0	0.0163
0.05	0.0508	0.00254	0.0168
0.10	0.0407	0.00407	0.0165
0.15	0.0308	0.00462	0.0155
0.20	0.0206	0.00412	0.0135
0.25	0.0108	0.00270	0.0103
0.305	0	0	0.0063
$B = 2$ $\beta_{0.75R} = 80^\circ$			
$\Omega R/V$	C_d	C_l	C_w
0.00	0.04	0	0.0345
2.40	0.148	0.355	
2.60	0.140	0.364	
2.80	0.132	0.370	0.792
3.00	0.124	0.372	0.807
3.20	0.116	0.371	0.817
3.40	0.108	0.367	0.822
3.60	0.101	0.364	0.826
3.80	0.0930	0.353	0.825
4.00	0.0861	0.344	0.824
4.20	0.0793	0.333	0.821
4.40	0.0726	0.319	0.816
4.60	0.0660	0.304	0.811
4.80	0.0590	0.283	0.804
5.00	0.0523	0.262	0.795
5.20	0.0457	0.238	0.786
5.40	0.0388	0.210	0.777
5.60	0.0319	0.179	0.767
5.80	0.0252	0.146	0.756
6.00	0.0185	0.111	0.746
6.20	0.0118	0.0732	0.735
6.40	0.0050	0.0320	0.725
6.54	0	0	0.717
$B = 3$ $\beta_{0.75R} = 10^\circ$			
$\Omega R/V$	C_d	C_l	C_w
0.00	0.0655	0	0.278
1.80	0.162	0.292	0.461
2.00	0.151	0.302	0.455
2.20	0.139	0.306	0.445
2.40	0.128	0.307	0.432
2.60	0.116	0.302	0.417
2.80	0.103	0.288	0.398
3.00	0.0900	0.270	0.377
3.20	0.0776	0.348	0.351
3.40	0.0647	0.220	0.323
3.60	0.0515	0.185	0.290
3.80	0.0383	0.146	0.249
4.00	0.0248	0.0992	0.200
4.20	0.0110	0.0462	0.148
4.30	0.0040	0.0172	0.120
4.355	0	0	0.105
$B = 3$ $\beta_{0.75R} = 20^\circ$			

which are drawn from these values become smoother. So, in this table, C_l , C_d , and C_w are written in three significant figures mostly.

TABLE 2 (*cont'd*)

$\Omega R/V$	C_d	C_l	C_w
0.00	0.0805	0	0.222
1.40	0.139	0.195	0.268
1.60	0.124	0.198	0.260
1.80	0.105	0.189	0.244
2.00	0.0840	0.168	0.215
2.20	0.0622	0.137	0.178
2.40	0.0400	0.0960	0.131
2.60	0.0175	0.0455	0.0800
2.70	0.0061	0.0165	0.0526
2.754	0	0	0.0370

$B = 3$
 $\beta_{0.75R} = 30^\circ$

$\Omega R/V$	C_d	C_l	C_w
0.00	0.0960	0	0.199
0.80	0.157	0.126	0.213
1.00	0.131	0.131	0.197
1.20	0.104	0.125	0.172
1.40	0.0755	0.106	0.142
1.60	0.0460	0.0736	0.103
1.80	0.0145	0.0261	0.0470
1.89	0	0	0.0175

$B = 3$
 $\beta_{0.75R} = 40^\circ$

$\Omega R/V$	C_d	C_l	C_w
0.00	0.0985	0	0.124
0.50	0.142	0.0710	0.126
0.60	0.127	0.0762	0.121
0.70	0.112	0.0784	0.115
0.80	0.0953	0.0762	0.106
0.90	0.0790	0.0711	0.0938
1.00	0.0622	0.0622	0.0792
1.10	0.0448	0.0493	0.0611
1.20	0.0261	0.0313	0.0390
1.30	0.0074	0.0096	0.0150
1.34	0	0	0.0055

$B = 3$
 $\beta_{0.75R} = 50^\circ$

$\Omega R/V$	C_d	C_l	C_w
0.00	0.103	0	0.0970
0.30	0.136	0.0408	0.0870
0.40	0.115	0.0460	0.0821
0.50	0.0935	0.0468	0.0748
0.60	0.0720	0.0432	0.0635
0.70	0.0508	0.0356	0.0490
0.80	0.0294	0.0235	0.0315
0.90	0.0080	0.0072	0.0130
0.94	0	0	0.0055

$B = 3$
 $\beta_{0.75R} = 60^\circ$

$\Omega R/V$	C_d	C_l	C_w
0.00	0.145	0	0.0512
0.10	0.121	0.0121	0.0485
0.20	0.0960	0.0192	0.0432
0.30	0.0715	0.0215	0.0355
0.40	0.0470	0.0188	0.0250
0.50	0.0222	0.0111	0.0128
0.59	0	0	0.0015

$B = 3$
 $\beta_{0.75R} = 70^\circ$

$\Omega R/V$	C_d	C_l	C_w
0.00	0.0785	0	0.0267
0.04	0.0682	0.00273	0.0251
0.08	0.0580	0.00464	0.0234
0.12	0.0476	0.00571	0.0214
0.16	0.0376	0.00602	0.0186
0.20	0.0273	0.00546	0.0148
0.24	0.0170	0.00408	
0.28	0.0069	0.00193	
0.307	0	0	

$B = 3$
 $\beta_{0.75R} = 80^\circ$

TABLE 2 (cont'd)

$\Omega R/V$	C_a	C_l	C_w
0.0	0.0515	0	0.450
2.0	0.184	0.368	0.892
2.2	0.167	0.367	0.900
2.4	0.154	0.370	0.910
2.6	0.146	0.380	0.924
2.8	0.137	0.384	0.934
3.0	0.129	0.387	0.942
3.2	0.121	0.387	0.948
3.4	0.113	0.384	0.957
3.6	0.105	0.378	0.963
3.8	0.0966	0.367	0.966
4.0	0.0885	0.354	0.967
4.3	0.0764	0.329	0.960
4.6	0.0639	0.294	0.940
4.9	0.0516	0.253	0.911
5.2	0.0392	0.204	0.877
5.5	0.0262	0.144	0.850
6.0	0.0035	0.021	0.835
6.07	0	0	0.833

$B = 4$
 $\beta_{0.75R} = 10^\circ$

$\Omega R/V$	C_a	C_l	C_w
0.0	0.090	0	0.481
1.8	0.194	0.349	0.615
2.0	0.178	0.356	0.607
2.2	0.163	0.359	0.593
2.4	0.148	0.355	0.572
2.6	0.132	0.343	0.545
2.8	0.117	0.328	0.515
3.0	0.101	0.303	0.483
3.2	0.0857	0.274	0.447
3.4	0.0702	0.239	0.403
3.6	0.0545	0.196	0.361
3.8	0.0390	0.148	0.328
4.0	0.0233	0.0932	0.307
4.2	0.0075	0.0315	0.302
4.291	0	0	

$B = 4$
 $\beta_{0.75R} = 20^\circ$

$\Omega R/V$	C_a	C_l	C_w
0.0	0.198	0	0.326
1.0	0.222	0.222	0.409
1.2	0.201	0.241	0.405
1.4	0.178	0.249	0.391
1.6	0.154	0.246	0.364
1.8	0.129	0.232	0.332
2.0	0.105	0.210	0.292
2.2	0.0787	0.173	0.244
2.4	0.0490	0.118	0.184
2.6	0.0225	0.0450	0.115

$B = 4$
 $\beta_{0.75R} = 30^\circ$

$\Omega R/V$	C_a	C_l	C_w
0.8	0.198	0.158	0.282
1.0	0.163	0.163	0.251
1.2	0.128	0.154	0.220
1.4	0.0930	0.130	0.180
1.6	0.0578	0.0925	0.125
1.8	0.0228	0.0410	0.0660
1.9	0.0048	0.0091	0.0345
1.926	0	0	

$B = 4$
 $\beta_{0.75R} = 40^\circ$

$\Omega R/V$	C_a	C_l	C_w
0.0	0.135	0	0.189
0.5	0.190	0.0950	0.147
0.6	0.167	0.100	0.170
0.7	0.145	0.102	0.166
0.8	0.123	0.0984	0.151
0.9	0.100	0.0960	0.132
1.0	0.0780	0.0780	0.109
1.1	0.0550	0.0605	0.0830
1.2	0.0325	0.0390	0.0555
1.3	0.0100	0.0130	0.0270
1.345	0	0	

$B = 4$
 $\beta_{0.75R} = 50^\circ$

TABLE 2 (*ccnt'd*)

$\Omega R/V$	C_d	C_l	C_w
0.0	0.133	0	0.129
0.5	0.125	0.0625	0.107
0.6	0.0960	0.0576	0.0912
0.7	0.0685	0.0480	0.0697
0.8	0.0403	0.0322	0.0451
0.9	0.0125	0.0113	
0.945	0	0	
$B = 4$ $\beta_{0.75R} = 60^\circ$			
$\Omega R/V$	C_d	C_l	C_g
0.25	0.109	0.0273	0.0611
0.30	0.0920	0.0276	0.0555
0.35	0.0750	0.0263	0.0492
0.40	0.0575	0.0230	0.0424
0.45	0.0404	0.0182	0.0346
0.50	0.0259	0.0130	0.0261
0.55	0.0135	0.0074	0.0173
0.60	0.0017	0.0010	0.0084
0.606	0	0	0.0074
$B = 4$ $\beta_{0.75R} = 70^\circ$			
$\Omega R/V$	C_d	C_l	C_w
0.00	0.110	0	0.0354
0.04	0.0950	0.0038	0.0351
0.08	0.0800	0.0064	0.0340
0.12	0.0655	0.0079	0.0314
0.16	0.0512	0.0082	0.0272
0.20	0.0372	0.0074	0.0218
0.24	0.0243	0.0058	0.0146
0.28	0.0124	0.00350	
0.32	0.0005	0.00016	
0.322	0	0	
$B = 4$ $\beta_{0.75R} = 80^\circ$			
$\Omega R/V$	C_d	C_l	C_w
0.0	0.088	0	0.0710
1.6	0.224	0.358	1.136
1.8	0.206	0.371	1.143
2.0	0.188	0.376	1.145
2.2	0.171	0.376	1.142
2.4	0.154	0.370	1.138
2.6	0.139	0.361	1.132
2.8	0.125	0.350	1.125
3.0	0.114	0.342	1.115
3.2	0.105	0.336	1.105
3.4	0.0970	0.330	1.095
3.6	0.0890	0.320	1.085
3.8	0.0810	0.308	1.078
4.0	0.0726	0.290	1.072
4.2	0.0641	0.269	1.065
4.4	0.0556	0.245	1.058
4.6	0.0470	0.216	1.052
4.8	0.0382	0.183	
5.0	0.0287	0.144	
5.2	0.0185	0.0962	
5.4	0.0070	0.0378	
5.5	0	0	
$B = 6$ $\beta_{0.75R} = 10^\circ$			
$\Omega R/V$	C_d	C_l	C_w
0.0	0.148	0	0.623
1.2	0.292	0.350	0.837
1.4	0.273	0.382	0.843
1.6	0.253	0.405	0.837
1.8	0.234	0.421	0.825
2.0	0.214	0.428	0.806
2.2	0.195	0.429	0.782
2.4	0.175	0.420	0.750
2.6	0.157	0.408	0.716
2.8	0.137	0.384	0.677
3.0	0.118	0.354	0.635
3.2	0.0989	0.316	0.588
3.4	0.0795	0.270	0.536
3.6	0.0600	0.216	0.478
3.8	0.0405	0.154	0.415
4.0	0.0230	0.0920	0.345
4.2	0.0085	0.0357	0.294
4.32	0	0	0.290
$B = 6$ $\beta_{0.75R} = 20^\circ$			

TABLE 2 (cont'd)

$\Omega R/V$	C_d	C_l	C_w
0.0	0.2	0	0.55
1.0	0.259	0.259	0.611
1.2	0.238	0.286	0.592
1.4	0.212	0.297	0.561
1.6	0.183	0.293	0.516
1.8	0.153	0.275	0.456
2.0	0.123	0.246	0.392
2.2	0.0910	0.200	0.323
2.4	0.0590	0.142	0.246
2.6	0.0270	0.0702	0.160
2.7	0.0110	0.0297	0.119
2.765	0	0	0.090

$B = 6$
 $\beta_{0.75R} = 30^\circ$

$\Omega R/V$	C_d	C_l	C_w
0.0	0.230	0	0.414
1.0	0.226	0.226	0.327
1.2	0.176	0.211	0.305
1.4	0.127	0.178	0.253
1.6	0.0775	0.124	0.179
1.8	0.0280	0.0504	0.0770
1.912	0	0	0

$B = 6$
 $\beta_{0.75R} = 40^\circ$

$\Omega R/V$	C_d	C_l	C_w
0.0	0.220	0	0.328
0.6	0.214	0.128	
0.7	0.189	0.132	0.219
0.8	0.163	0.130	0.201
0.9	0.136	0.122	0.178
1.0	0.109	0.109	0.150
1.1	0.0810	0.0891	0.118
1.2	0.0518	0.0622	0.0840
1.33	0	0	

$B = 6$
 $\beta_{0.75R} = 50^\circ$

$\Omega R/V$	C_d	C_l	C_w
0.2	0.280	0.0560	0.180
0.3	0.243	0.0729	0.168
0.4	0.204	0.0816	0.153
0.5	0.167	0.0835	0.135
0.6	0.129	0.0774	0.113
0.7	0.0910	0.0637	0.0860
0.8	0.0530	0.0424	0.0570
0.9	0.0150	0.0135	
0.94	0	0	

$B = 6$
 $\beta_{0.75R} = 60^\circ$

$\Omega R/V$	C_d	C_l	C_w
0.0	0.260	0	0.103
0.1	0.215	0.0215	0.100
0.2	0.172	0.0344	0.0914
0.3	0.129	0.0387	0.0750
0.4	0.0852	0.0341	0.0554
0.5	0.0420	0.0210	0.0359
0.596	0	0	0.0176

$B = 6$
 $\beta_{0.75R} = 70^\circ$

$\Omega R/V$	C_d	C_l	C_w
0.00	0.151	0	0.0440
0.05	0.126	0.0063	0.0438
0.10	0.102	0.0102	0.0424
0.15	0.0780	0.0117	0.0385
0.20	0.0528	0.0106	0.0312
0.25	0.0280	0.0070	0.0234
0.30	0.0038	0.0011	0.0175
0.309	0	0	0.0165

$B = 6$
 $\beta_{0.75R} = 80^\circ$

TABLE 2 (cont'd)

$\Omega R/V$	C_d	C_l	C_w
0.0	0.0550	0	0.113
0.8			0.150
1.0	0.112	0.112	0.160
1.2	0.0888	0.107	0.146
1.4	0.0646	0.0904	0.114
1.6	0.0397	0.0635	0.0710
1.8	0.0130	0.0234	0.0349
1.9	0	0	0.0262

$B = 2$
 $\beta_{0.75R} = 40^\circ$
 With ring

$\Omega R/V$	C_d	C_l	C_w
0.0	0.0599	0	
0.6	0.114	0.0684	0.110
0.7	0.100	0.0700	0.105
0.8	0.0855	0.0684	0.0960
0.9	0.0700	0.0630	0.0815
1.0	0.0538	0.0538	0.0663
1.1	0.0370	0.0407	0.0500
1.2	0.0205	0.0246	0.0330
1.325	0	0	0.0110

$B = 2$
 $\beta_{0.75R} = 50^\circ$
 With ring

$\Omega R/V$	C_d	C_l	C_w
0.0	0.0595	0	
0.4	0.104	0.0416	0.0799
0.5	0.0835	0.0418	0.0712
0.6	0.0640	0.0384	0.0599
0.7	0.0435	0.0305	0.0449
0.8	0.0220	0.0176	0.0268
0.90	0	0	0.0100

$B = 2$
 $\beta_{0.75R} = 60^\circ$
 With ring

$\Omega R/V$	C_d	C_l	C_w
0.2	0.0870	0.0174	0.0485
0.3	0.0646	0.0194	0.0399
0.4	0.0420	0.0168	0.0298
0.5	0.0197	0.0099	0.0180
0.605	0	0	0.0050

$B = 2$
 $\beta_{0.75R} = 70^\circ$
 With ring

$\Omega R/V$	C_d	C_l	C_w
0.0	0.0839	0	0.155
1.0	0.153	0.153	0.207
1.2	0.122	0.146	0.188
1.4	0.0878	0.123	0.154
1.6	0.0523	0.0837	0.108
1.8	0.0153	0.0275	0.0525
1.885	0	0	0.0250

$B = 3$
 $\beta_{0.75R} = 40^\circ$
 With ring

$\Omega R/V$	C_d	C_l	C_w
0.0	0.0905	0	0.164
0.6	0.136	0.0816	0.160
0.7	0.126	0.0882	0.153
0.8	0.114	0.0912	0.143
0.9	0.0970	0.0873	0.130
1.0	0.0750	0.0750	0.111
1.1	0.0515	0.0567	0.0833
1.2	0.0265	0.0318	0.0500
1.3	0.0040	0.0052	0.0203
1.36	0	0	0.0135

$B = 3$
 $\beta_{0.75R} = 50^\circ$
 With ring

$\Omega R/V$	C_d	C_l	C_w
0.0	0.0850	0	0.0910
0.4	0.137	0.0548	0.0898
0.5	0.109	0.0545	0.0837
0.6	0.0825	0.0495	0.0735
0.7	0.0560	0.0392	0.0556
0.8	0.0295	0.0236	0.0360
0.9	0.0035	0.0315	0.0150
0.912	0	0	0.0120

$B = 3$
 $\beta_{0.75R} = 60^\circ$
 With ring

$\Omega R/V$	C_d	C_l	C_w
0.0	0.118	0	0.0610
0.2	0.125	0.0250	0.0637
0.3	0.0920	0.0276	0.0557
0.4	0.0585	0.0234	0.0424
0.5	0.0246	0.0123	0.0258
0.6	0	0	0.0080

$B = 3$
 $\beta_{0.75R} = 70^\circ$
 With ring

TABLE 2 (cont'd)

$\Omega R/V$	C_d	C_t	C_w	$\Omega R/V$	C_d	C_t	C_w
0.0	0.121	0	0.235	0.0	0.123	0	0.125
1.0	0.175	0.175	0.263	0.4	0.179	0.0716	0.146
1.2	0.135	0.162	0.239	0.5	0.146	0.0730	0.129
1.4	0.0959	0.134	0.192	0.6	0.112	0.0672	0.106
1.6	0.0560	0.0896	0.130	0.7	0.0780	0.0546	0.0806
1.8	0.0198	0.0356	0.0597	0.8	0.0437	0.0356	0.0532
1.927	0	0	0.0300	0.9	0.0010	0.0009	0.0219
				0.930	0	0	0.0110
$B = 4$ $\beta_{0.75R} = 40^\circ$ With ring				$B = 4$ $\beta_{0.75R} = 60^\circ$ With ring			
$\Omega R/V$	C_d	C_t	C_w	$\Omega R/V$	C_d	C_t	C_w
0.8	0.154	0.123	0.199	0.1	0.189	0.0189	0.0815
0.9	0.125	0.113	0.178	0.2	0.149	0.0298	0.0736
1.0	0.0965	0.0965	0.149	0.3	0.107	0.0321	0.0624
1.1	0.0675	0.0743	0.117	0.4	0.0710	0.0284	0.0482
1.2	0.0387	0.0464	0.0815	0.5	0.0360	0.0180	0.0306
1.3	0.0105	0.0137	0.0455	0.6	0.0010	0.0006	0.0115
1.34	0	0	0.0324	0.605	0	0	
$B = 4$ $\beta_{0.75R} = 50^\circ$ With ring				$B = 4$ $\beta_{0.75R} = 70^\circ$ With ring			

The full lines show the performances of windmills alone and the dotted lines are for the windmills with rings.

The symbols used in these Figures are as follows.

$\frac{\Omega R}{V}$	the ratio of the peripheral speed of windmills to the wind velocity,
$G_d = \frac{Q}{\frac{1}{2}\rho V^2 \pi R^3}$	torque coefficient of windmills,
$C_w = \frac{D}{\frac{1}{2}\rho V^2 \pi R^2}$	drag coefficient of windmills,
$C_t = \frac{P}{\frac{1}{2}\rho V^3 \pi R^3}$	power coefficient of windmills, $C_t = C_d \frac{\Omega R}{V}$,
ρ	air density ($\text{kg sec}^2/\text{m}^4$),
Ω	angular velocities of windmills (radian/sec),
D	drag force of windmills (kg),
P	power of windmills (kg m/sec),
Q	torque of windmills (kg m),
R	radius of windmills (m),
V	wind velocity (m/sec).

The wind velocity is between 8 m/sec and 20 m/sec, and the Reynolds number at the section of 75 per cent of radius is about within 1×10^5 and 2×10^5 , where the chord length of the airfoil c is taken as the length, and the velocity is represented by the resultant velocity W_1 (see Figure 17).

In the experiments of the blade angle of 80° and 70° the drag coefficients which were measured in different torque weight W (see Figure 1) were different from each other. When the torque weight W was large the drag coefficient showed a lower value, the cause of which is partially the coming in of the torque component force into the drag component, and the calibration for this error is made in all the data, but the difference between the measured values of C_w in various values of W cannot be covered by this calibration, so that the C_w curves for 70° and 80° shown in Figures 6, 9, 12 and 15 are the mean values of these different test results.

In the low angles of 10° and 20° , the C_d and C_w curves for the four and six bladed windmills showed the various but continuous curves, when they were measured by regulating the wind velocity under the constant torque weight W . This unstable character vanished when the torque was measured by varying the torque weight W at the constant wind velocity. The curves for 10° and 20° of the three, four and six bladed windmills were obtained in this manner. But even by this method, the curves of C_d and C_w of the four bladed windmills showed some instability and the author could not obtain the exact points of experiments between $\Omega R/V = 2.3$ and 4.0 at the blade angle of 10° , so the corresponding curves in Figures 10, 11 and 12 are drawn by the dotted lines. In the two bladed windmill any instability could not be seen. In the three bladed windmill a little instability occurred, but it was not so remarkable as in the four bladed windmill. In the four bladed windmill the most unstable characters were experienced, while this became small in the six bladed windmill. The cause of the above phenomena is not yet clear. But some part of the phenomena may be attributed to the low Reynolds number of these experiments. On the other hand some instability may exist in the flow around the airfoils which are arranged to form a lattice of airfoils with high angle of stagger, for the curves of C_d of 10° in Figures 10 and 13 are bent sharply at a certain values of $\Omega R/V$, and the points where C_d becomes to zero becomes smaller. These changes of slopes and zero points show the effect of lattice of airfoils, therefore it may be supposed that the airfoil elements are affected by the effect of lattice especially at this blade angle.

As can be seen in Figures 5, 8, 11 and 14, by decreasing the angle of blades, the power coefficient increases very much, but when the angle is reduced below 20° , the rate of increase in C_l becomes small. This trend is more remarkable at the higher number of blades, and in the case of the six bladed windmill the curve of C_d of 10° is below the curve of 20° at the interval of $\Omega R/V = 0 \sim 2.8$, so that C_l curve also shows the lower value than the one of 20° . The further reduction of angle will result in the decrease of C_l . Sanuki performed experiments beyond this angle, which was called 'critical angle' by him.

From the results stated above it may be said that by reducing the angle of blades down to some angle the power of windmills increases, but below this angle the windmill shows some unstable motion and the power becomes smaller. So the blades of windmills must be set at appropriate angles above the critical and unstable angles. The critical angle exists below 10° in the author's experiment, but even above this value of angle the instability of performances occurs. Accordingly, if this instability of performances occurs in full scale windmills, it will be necessary to set the blade above 20° for the four and six bladed fast running windmills.

The drag coefficient increases rapidly when the angle of blades becomes smaller than 30° (see Figures 6, 9, 12 and 15). To avoid this high resistance of windmills the blade angle is desired to be larger than 30° . Considering both the critical angle and the rapid increase of the blade angle in the fast running windmills with more number of blades than four, it is reasonable to set the blades at about between 20° and 30° . In the cases of two or three bladed windmills the value is smaller than 20° , but considering the increase of the drag, the angle should be set to be larger than 10° .

On the other hand, as seen in Figures 5, 8, 11 and 14, in the fast running windmills having low angle of blades, the maximums of C_l are not affected by the increase of the number of blades, and when the number of blades is increased more than three, the value of $C_{l\max}$ is about 0.35. So the most suitable fast running windmill is the three bladed windmill in the author's experiment. This result agrees with Sanuki's ones. But when the strong starting torque is required, the many bladed windmills such as four or six bladed ones are preferable to the three bladed windmill.

The performances of windmills with rings are also shown in Figures 4–12. The distances between the tips of the windmills and the ring were in average 10 mm ~ 13 mm. The tips of the windmills form the true circular arc at the blade angle of 40° , so that the clearance between the tips and the ring becomes smaller in the lower angles than 40° . The experiment was restricted to the larger blade angles than 40° , because at the lower blade angles than this the tips of the windmills contacted with the ring. The C_d , C_l and C_w are increased by attaching the ring and the increment is larger as the blade angle becomes higher and the number of blades decreases, and the increment are at most 30 per cent. In Sanuki's experiment⁸⁾ the increment by the duct tube is very large, and from the author's experiments it became clear that the results of Sanuki are due to mainly the acceleration of the wind velocity by the ventilator tube.

4. Formulas for the calculation of the performances of windmills.

Lock⁹⁾ gives a simple formula for the calculation of the induced velocity of propellers by using the Goldstein's solution of the flow around rigid helical

⁸⁾ M. Sanuki: *loc. cit.*, pp. 284–286.

⁹⁾ C. N. H. Lock and D. Yeatman: Tables for Use in an Improved Method of Airscrew Strip Theory Calculation, Report and Memoranda No. 1674, 1953–36, Vol. 1, pp. 254–261.

vortex sheets, and represents the effect of pitch of the helical surface and the number of blades by the factor κ . By him the induced velocity at the blade element of propellers w is given by

$$(1) \quad w = \frac{s C_L W_1'}{4 \kappa \sin \phi},$$

TABLE 3. Value of κ

(from C. N. H. Lock and D. Yeatman: Tables for Use in an Improved Method of Airscrew Strip Theory Calculation, *R & M*, No. 1674, pp. 270-280.)

r/R $\sin \phi$	0.3	0.45	0.6	0.7	0.75	0.8	0.85	0.9	0.95
0.05	1.000	1.000	1.000	0.999	0.997	0.994	0.985	0.950	0.780
0.1	1.000	0.998	0.997	0.988	0.971	0.937	0.877	0.773	0.586
0.2	0.994	0.991	0.961	0.901	0.852	0.784	0.694	0.578	0.415
0.3	0.978	0.959	0.874	0.774	0.709	0.634	0.548	0.444	0.308
0.4	0.958	0.906	0.783	0.663	0.595	0.520	0.442	0.351	0.243
0.5	0.944	0.848	0.690	0.564	0.501	0.434	0.367	0.289	0.199
0.6	0.930	0.784	0.608	0.492	0.435	0.376	0.316	0.249	0.171
0.7	0.922	0.722	0.547	0.441	0.387	0.333	0.278	0.218	0.149
0.8	0.916	0.677	0.502	0.398	0.347	0.297	0.247	0.193	0.131
0.9	0.935	0.657	0.464	0.360	0.311	0.265	0.220	0.172	0.117
1.0	1.012	0.633	0.425	0.325	0.279	0.238	0.197	0.154	0.105

Values of κ for two-bladed windmills or propellers.

r/R $\sin \phi$	0.3	0.45	0.6	0.7	0.75	0.8	0.85	0.9	0.95
0.05	1.000	1.000	1.000	1.000	0.999	0.998	0.990	0.973	0.863
0.1	1.000	0.999	0.999	0.998	0.994	0.980	0.948	0.872	0.692
0.2	0.997	0.995	0.988	0.964	0.935	0.884	0.810	0.693	0.512
0.3	0.992	0.987	0.955	0.892	0.843	0.774	0.684	0.566	0.406
0.4	0.984	0.966	0.902	0.809	0.746	0.670	0.581	0.471	0.331
0.5	0.975	0.940	0.836	0.725	0.658	0.581	0.496	0.396	0.275
0.6	0.973	0.909	0.771	0.650	0.582	0.508	0.429	0.341	0.236
0.7	0.983	0.880	0.714	0.586	0.520	0.450	0.377	0.299	0.203
0.8	1.010	0.849	0.661	0.533	0.470	0.404	0.337	0.265	0.182
0.9	1.061	0.831	0.622	0.494	0.429	0.367	0.304	0.239	0.164
1.0	1.185	0.832	0.588	0.457	0.393	0.335	0.278	0.218	0.149

Values of κ for three-bladed windmills or propellers.

r/R $\sin \phi$	0.3	0.45	0.6	0.7	0.75	0.8	0.85	0.9	0.95
0.05	1.000	1.000	1.000	1.000	1.000	0.999	0.998	0.995	0.945
0.1	1.000	1.000	1.000	1.000	0.999	0.993	0.985	0.943	0.770
0.2	0.998	0.997	0.995	0.989	0.973	0.940	0.882	0.777	0.590
0.3	0.996	0.994	0.984	0.945	0.909	0.852	0.774	0.651	0.476
0.4	0.991	0.984	0.950	0.883	0.830	0.759	0.671	0.554	0.396
0.5	0.985	0.971	0.905	0.812	0.750	0.674	0.585	0.476	0.334
0.6	0.986	0.954	0.855	0.745	0.678	0.601	0.517	0.414	0.290
0.7	0.999	0.939	0.803	0.682	0.615	0.541	0.459	0.369	0.255
0.8	1.035	0.924	0.756	0.627	0.562	0.490	0.413	0.329	0.228
0.9	1.103	0.917	0.713	0.581	0.516	0.447	0.375	0.298	0.205
1.0	1.256	0.923	0.681	0.543	0.477	0.412	0.345	0.272	0.187

Values of κ for four-bladed windmills or propellers.

where

W_1' resultant wind velocity (see Figure 17),

$s = \frac{Bc}{2\pi r}$ the solidity of the blade element,

B blade number,

C_L lift coefficient of airfoil,

κ coefficient showing the effect of finite blade number.

This is the function of r/R , B and ϕ , where r is the radius of blade element, and ϕ is the pitch angle of vortex sheet on the windmill plane. κ is tabulated in Table 3 and shown in curves in Figure 16(a), (b) and (c).

Without any further considerations, Equation (1) is applicable to the cases of windmills by simply reversing the sign of w . On the other hand, the lift coefficient C_L is given by

$$C_L = 2\pi k \sin \alpha_e \div 2\pi k \alpha_e = 2\pi (\alpha - \alpha_i), \quad (2)$$

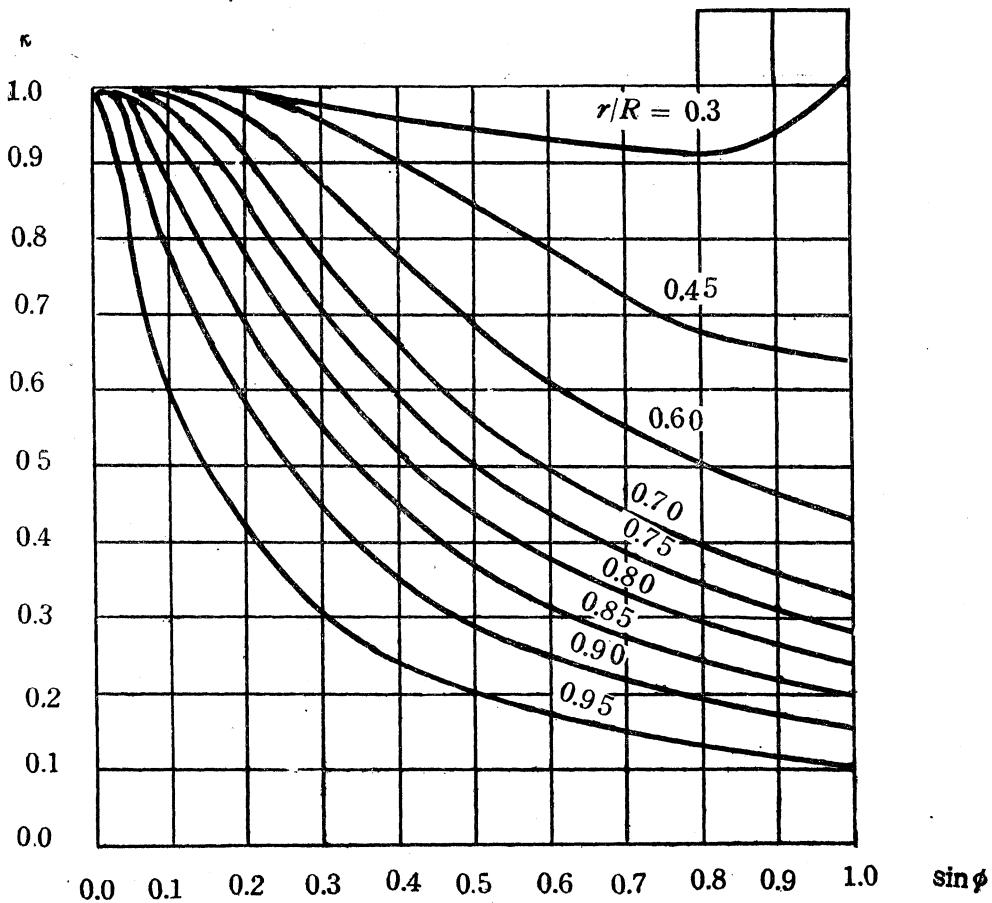


FIG. 16(a). The curves of κ for two bladed windmills or propellers.

where

$k = \frac{1}{2\pi} \frac{dC_L}{d\alpha}$ slope of lift coefficient of two dimensional airfoil divided by 2π ,

α_e effective angle of attack (radian)

α geometrical angle of attack of the elemental airfoil at the radius r measured from the none lift axis of the blade element (radian).

α_i induced angle of attack (radian).

The lift coefficient is generally related to the circulation Γ around the blade element by

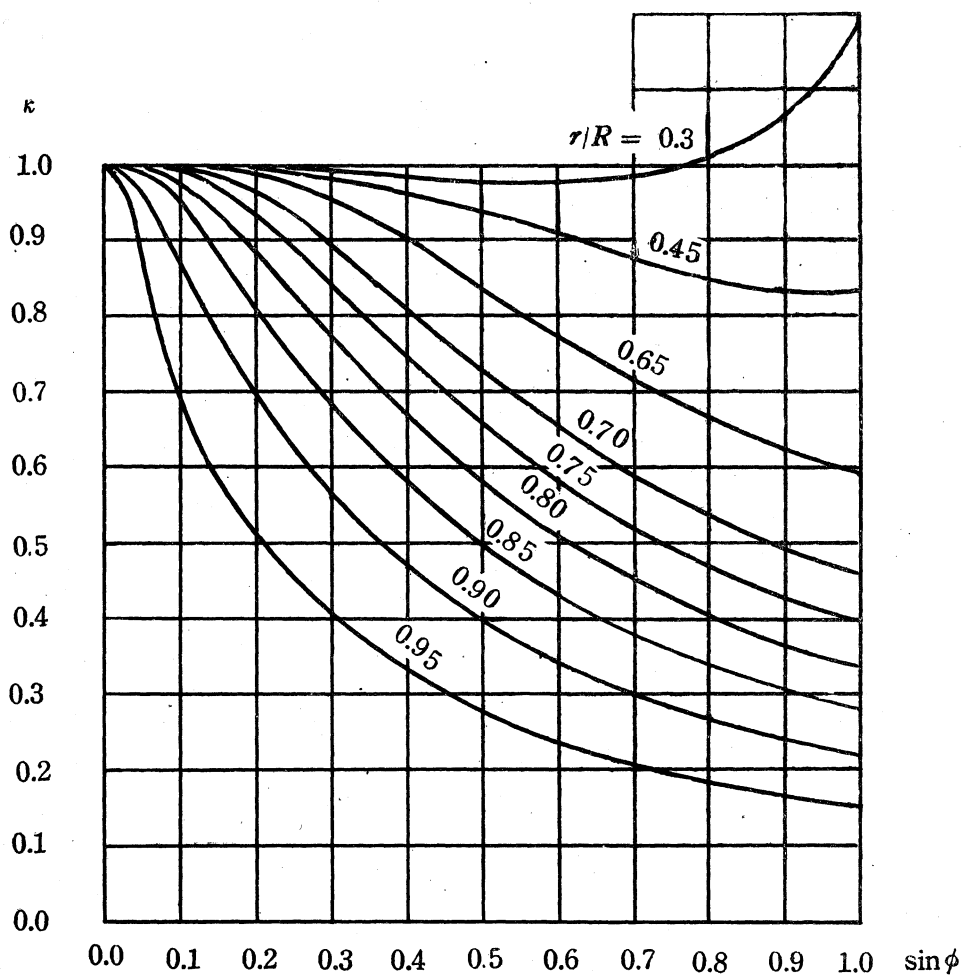


FIG. 16(b). The curves of κ for three bladed windmills or propellers.

$$C_L = \frac{2 I'}{c W_1'}, \quad (3)$$

where c is the chord length of the blade element. As can be seen from Figure 17, W_1' is given by

$$W_1' = W_1 \cos \alpha_i = V \sqrt{1 + \mu^2} \cos \alpha_i, \quad \text{where } \mu = \Omega r / V. \quad (4)$$

From Equations (3) and (4) we obtain

$$C_L = \left(\frac{B I'}{\pi V R} \right) \frac{1}{s \left(\frac{r}{R} \right) \sqrt{1 + \mu^2} \cos \alpha_i}. \quad (5)$$

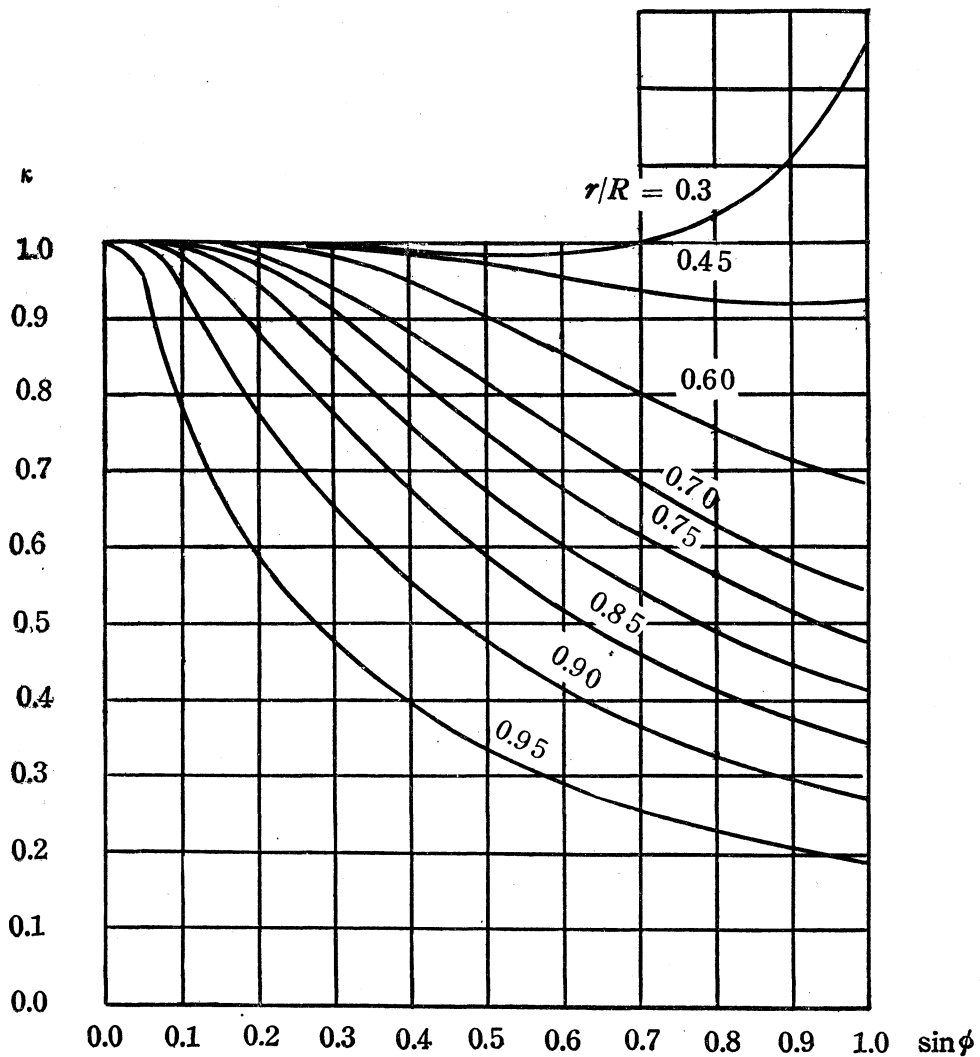


FIG. 16(c). The curves of κ for four bladed windmills or propellers.

The induced angle of attack α_i is approximately written in the form

$$\alpha_i = \frac{w}{W_1}. \quad (6)$$

From Equations (1), (5) and (6) we get

$$\alpha_i = \left(\frac{B \Gamma}{\pi V R} \right) \frac{1}{4 \kappa \left(\frac{r}{R} \right) \sqrt{1 + \mu^2} \sin \phi}. \quad (7)$$

Substituting Equations (7) and (5) in Equation (2), we obtain the following equation.

$$\left(\frac{B \Gamma}{\pi V R} \right) \frac{1}{s \left(\frac{r}{R} \right) \sqrt{1 + \mu^2} \cos \alpha_i} = 2 \pi k \left\{ \alpha - \left(\frac{B \Gamma}{\pi V R} \right) \frac{1}{4 \kappa \left(\frac{r}{R} \right) \sqrt{1 + \mu^2} \sin \phi} \right\}. \quad (8)$$

Solving this equation we get

$$\left(\frac{B \Gamma}{\pi V R} \right) = \frac{4 \alpha \left(\frac{r}{R} \right) \pi k s \kappa \sqrt{1 + \mu^2} \cos \alpha_i \sin \phi}{2 \kappa \sin \phi + \pi k s \cos \alpha_i}. \quad (9)$$

The induced angle of attack α_i is given by Equation (7). Then the pitch angle ϕ is

$$\phi = \theta - \alpha_i, \quad \text{where } \theta = \tan^{-1} \mu, \quad (10)$$

and the effective angle of attack is calculated from

$$\alpha_e = \alpha - \alpha_i. \quad (11)$$

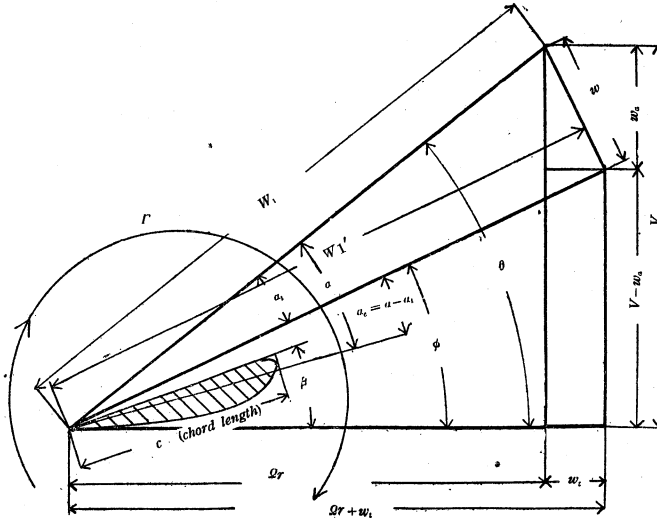


FIG. 17. The wind speed diagram for the blade element at radius r .

When the α_e is known, the C_L can be found from Equation (2). Using the values obtained from the above equations, the torque, power and drag coefficients of windmills are calculated by the following formulas:

$$\left. \begin{aligned}
 C_w &= \frac{\rho \left[\int_{\text{boss}}^{\text{tip}} \left\{ B I' (\Omega r + w_t) + \frac{1}{2} B c C_D W_1'^2 \sin \phi \right\} dr \right]}{\frac{1}{2} \rho V^2 \pi R^2} \\
 &= 2 \int_{(r/R)_{\text{boss}}}^1 \left[\left(\frac{B I'}{\pi V R} \right) \sqrt{1 + \mu^2} \cos \alpha_i \cos \phi \right. \\
 &\quad \left. + s C_D (1 + \mu^2) \left(\frac{r}{R} \right) \cos^2 \alpha_i \sin \phi \right] d \left(\frac{r}{R} \right), \\
 C_d &= \frac{\rho \left[\int_{\text{boss}}^{\text{tip}} \left\{ B I' (V - w_a) - \frac{1}{2} B c C_D W_1'^2 \cos \phi \right\} r dr \right]}{\frac{1}{2} \rho V^2 \pi R^3} \\
 &= 2 \int_{(r/R)_{\text{boss}}}^1 \left[\left(\frac{B I'}{\pi V R} \right) \sqrt{1 + \mu^2} \cos \alpha \sin \phi \right. \\
 &\quad \left. - s C_D (1 + \mu^2) \left(\frac{r}{R} \right) \cos^2 \alpha_i \cos \phi \right] \left(\frac{r}{R} \right) d \left(\frac{r}{R} \right), \\
 C_l &= C_a \frac{\Omega R}{V},
 \end{aligned} \right\} \quad (12)$$

where

- C_D drag coefficient of two-dimensional airfoils,
- w_t tangential component of induced velocity w (see Figure 17),
- w_a axial component of induced velocity w (see Figure 17).

The procedure of the calculation of the performances of windmills is as follows.

As the first approximation we may put $\phi = \theta$ or $\alpha_i = 0$. Then the Equations (9), (7), (10), (2) and (5) are reduced to

$$\left(\frac{B I'}{\pi V R} \right)_1 = \frac{4 \alpha \left(\frac{r}{R} \right) \pi k s \kappa \sqrt{1 + \mu^2}}{2 \kappa + \pi k s \sqrt{1 + \mu^2}}, \quad (13)$$

$$\alpha_{i1} = \left(\frac{B I'}{\pi V R} \right)_1 \frac{1}{4 \kappa \left(\frac{r}{R} \right)}, \quad (14)$$

$$\phi_1 = \tan^{-1} \mu - \alpha_{i1}, \quad (15)$$

$$\alpha_{e1} = \alpha - \alpha_{i1}, \quad (16)$$

$$C_{L1} = 2 \pi k \alpha_{e1} = \left(\frac{B I'}{\pi V R} \right)_1 \frac{1}{s \left(\frac{r}{R} \right) \sqrt{1 + \mu^2}}. \quad (17)$$

TABLE 4.

r/R	μ	θ''	$\beta^\circ-5.35^\circ$	α°	s	κ	$\left(\frac{B\Gamma}{\pi VR}\right)_1$	α_{i1}°	ϕ_{i1}''
	$= \frac{r}{R} \frac{\Omega R}{V}$	$= \cot^{-1} \mu$	from zero lift axis	$= \theta^\circ - \beta^\circ + 5.35^\circ$	$= \frac{cB}{2\pi r}$	$\sin \phi = \sin \theta, \frac{r}{R}$ Fig. 16(c)	Eq. (13)	Eq. (14)	Eq. (15)
0.34	0.85	49° 33'	34.12°	15.51°	0.574	1.001	0.178	7.47°	42° 10'
0.4	1.00	45° 00'	30.32°	14.68°	0.490	0.967	0.198	7.32°	37° 41'
0.6	1.50	33° 00'	20.17°	13.51°	0.333	0.878	0.242	6.59°	27° 05'
0.75	1.875	28° 04'	14.65°	13.42°	0.277	0.773	0.279	6.90°	21° 10'
0.85	2.125	25° 12'	11.77°	13.43°	0.255	0.647	0.290	7.55°	17° 39'
0.925	2.313	23° 23'	9.92°	13.46°	0.244	0.438	0.270	8.57°	14° 49'
0.975	2.438	22° 18'	8.83°	13.49°	0.241	0.268	0.188	10.32°	12° 00'

Conditions:

$$\Omega R/V = 2.5,$$

$$\beta_{0.75R} = 23^\circ,$$

$$B = 4,$$

It is convenient to write angles in radian except in the cases when they

For the second and the further approximation the formulas are

$$\left(\frac{B\Gamma}{\pi VR}\right)_n = \frac{4\alpha \left(\frac{r}{R}\right) \pi k s \kappa \sqrt{1+\mu^2} \cos \alpha_{i n-1} \sin \phi_{n-1}}{2\kappa_{n-1} \sin \phi_{n-1} + \pi k s \cos \alpha_{i n-1}}, \quad (18)$$

$$\alpha_n = \left(\frac{B\Gamma}{\pi VR}\right)_{n-1} \frac{1}{4\kappa_{n-1} \left(\frac{r}{R}\right) \sqrt{1+\mu^2} \sin \phi_{n-1}}, \quad (19)$$

$$\phi_n = \tan^{-1} \mu - \alpha_{in}, \quad (20)$$

$$\alpha_{en} = \alpha - \alpha_{in}, \quad (21)$$

$$C_{Ln} = 2\pi k \alpha_{en}, \quad (22)$$

where n is an integer larger than 2 which means the order of the approximation.

When $(B\Gamma/\pi VR)_n$ becomes almost equal to $(B\Gamma/\pi VR)_{n-1}$, then we need not to proceed to the higher approximation. But Goldstein's solution, which plays the fundamental rôle in Lock's Equation (1), is exact only when the w is small compared with W_1' , that is, only in the light loaded stated of windmills or propellers, so that the results will not generally a exact ones, even if the abovementioned approximation is proceeded to the higher order and the approximation converges. Consequently the approximation should be restricted within the second or third orders or $n \leq 3$ even in the heavy loaded atate.

κ_1	$\left(\frac{B\Gamma}{\pi VR}\right)_2$	α_{i2}°	ϕ_2°	α_{e2}°	C_{L2}	C_D	$R \frac{dC_w}{dr}$	$R \frac{dC_d}{dr}$
$\sin \phi_1, \frac{r}{R}$ Fig. 16(c)	Eq. (18)	Eq. (19)	Eq. (20)	Eq. (21)	Eq. (22)	$C_l \sim C_D$ curve	Eq. (23)	Eq. (23)
0.984	0.174	8.45°	41° 11'	7.06°	0.685	0.0135	0.344	0.100
0.970	0.183	7.81°	37° 11'	6.86°	0.666	0.0132	0.415	0.121
0.926	0.224	7.05°	26° 38'	6.46°	0.627	0.0127	0.725	0.207
0.862	0.256	7.39°	20° 41'	6.03	0.585	0.0124	1.018	0.270
0.771	0.233	8.07°	16° 57'	5.37°	0.521	0.0117	1.177	0.281
0.620	0.236	9.15°	14° 14'	4.31°	0.418	0.0110	1.145	0.239
0.422	0.167	10.62°	11° 42'	2.84°	0.276	0.0105	0.855	0.140

Plan form and pitch distribution: Table 1,

Airfoil section: Göttingen 623, (zero lift angle = $-5^\circ 21'$), Table 1,

$2\pi k = 5.56$.

are used to find the values of trigonometric functions.

C_w , C_d and C_l are calculated by the following equations:

$$\left. \begin{aligned}
 C_w &= 2 \int_{(r/R)_{\text{boss}}}^1 \left[\left(\frac{B\Gamma}{\pi VR} \right)_n \sqrt{1 + \mu^2} \cos \alpha_{in} \cos \phi_n \right. \\
 &\quad \left. + s C_D (1 + \mu^2) \left(\frac{r}{R} \right) \cos^2 \alpha_{in} \sin \phi_n \right] d \left(\frac{r}{R} \right), \\
 C_d &= 2 \int_{(r/R)_{\text{boss}}}^1 \left[\left(\frac{B\Gamma}{\pi VR} \right)_n \sqrt{1 + \mu^2} \cos \alpha_{in} \sin \phi_n \right. \\
 &\quad \left. - s C_D (1 + \mu^2) \left(\frac{r}{R} \right) \cos^2 \alpha_{in} \cos \phi_n \right] d \left(\frac{r}{R} \right), \\
 C_l &= C_d \frac{2R}{V}.
 \end{aligned} \right\} (23)$$

The example of calculation is given in Table 4.

The comparison of the results calculated by this method with the results of the author's experiment is tabulated in Table 5.

The agreement of these two kinds of values is considerably good in the torque and power coefficients, but the drag coefficients obtained by the experiment are about 10 per cent higher than the theoretical ones. The author interpretes that this discrepancy is due to the neglect of the pressure drag of the boss, and the using of the airfoil data obtained at Göttingen. For, neglecting the pressure drag of the boss, the drag of windmills is

TABLE 5. The comparison of the calculated values with the experimental ones.

(The upper values are the calculated values and the lower ones are obtained by the experiment, and these calculated values are obtained from the second approximation.)

The state of fast running windmills				The state of slow running windmills			
$\beta_{0.75R} = 20^\circ$				$\beta_{0.5R} = 60^\circ$			
$\Omega R/V = 2.5$				$\Omega R/V = 0.5$			
B	C_d	C_l	C_w	B	C_d	C_l	C_w
2	0.091	0.23	0.33	2	0.067	0.034	0.047
	0.095	0.24	0.36		0.068	0.034	0.059
3	0.119	0.30	0.45	3	0.094	0.047	0.068
	0.121	0.30	0.43		0.094	0.047	0.075
4	0.136	0.34	0.54	4	0.121	0.061	0.088
	0.140	0.35	0.56		0.125	0.063	0.107

overestimated as mentioned in paragraph 2, and the experiment in Göttingen is performed in $Re = 4 \times 10^5$, while the author's experiment is made at 1×10^5 or 2×10^5 at the airfoil of $r/R = 0.75$, so that the C_D of airfoils used in this calculation is too small.

To estimate the accuracy of the author's method, the performance of the SW-I propeller¹⁰⁾ calculated by his method is compared with Kawada's results of calculation and experiment. In the calculation of performance of propellers the signs attached to the second terms of Equations (12) and (23) must be reversed, and in Equations (10), (15) and (21) the sign before α_i be positive. The results of calculation are as follows:

C_T	C_P	η	
0.116	0.090	0.68	the author's method (the second app.)
0.122	0.093	0.69	Kawada's second approximation
0.122	0.092	0.68	Kawada's experiment

SW-I propeller,

$$B = 2,$$

$$\Omega R/V = 6, \text{ or } V/nD = 0.524,$$

$$C_T = (\text{thrust})/n^2 D^4,$$

$$C_P = (\text{power})/n^3 D^5,$$

$$\eta = \text{efficiency} = (C_T/C_P) (V/nD),$$

$$n = \text{number of revolution (r.p.s.)},$$

$$D = \text{diameter of propellers (m.)}.$$

¹⁰⁾ S. Kawada: Calculation of Induced Velocity by Helical Vortices and its Application to Propeller Theory, Report of the Aeronautical Research Institute, Tōkyō Imperial University, No. 172, Jan. 1939.

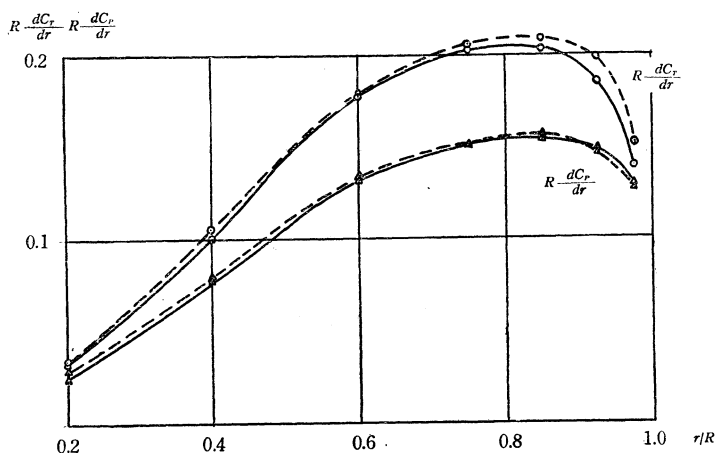


FIG. 18. The comparison of the results of calculation by the author's method with Kawada's results with regard to the distributions of $R(dC_p/dr)$ and $R(dC_T/dr)$ along the blade.

—— the author's method.
 ----- Kawada's method.

The comparison of torque and thrust distributions of SW-I propeller is shown in Figure 18. We cannot say that the agreement is so good, because propellers require high accuracy. But the author's method is sufficient to calculate the performances of windmills for which the accuracy of such degree is not necessary.

In the calculation of many bladed windmills, it will be necessary to consider the interference of two-dimensional airfoils as a lattice of airfoil. Abe¹¹⁾ calculated the performance of windmills having many blades under consideration of this effect, and obtained good agreement with the experiment.

The distributions of C_L along the blades which can be obtained by Equation (22) are shown in Figure 19. The working conditions of the windmills lie near the points of $C_{L \max}$. We see that in the high blade angle the blade number of windmills affects little the distribution of C_L along each blade, but in the low angle the increase of blade number yields the reduction of C_L , and hence the C_L at $C_{L \max}$ for the fast running windmills having many blades is smaller than the case of ones having small number of blades.

5. Analysis of windmills with a ring. The results of experiments of the windmills with rings does not show the exact performance affected by the ring of infinite length, for the ring which is attached to the windmill

¹¹⁾ Abe: On the Theory of Windmills (in Japanese), The Report of the Institute of High Speed Mechanics, Tôhoku University, Sendai, Japan, Vol. 5, No. 42, March 1951.

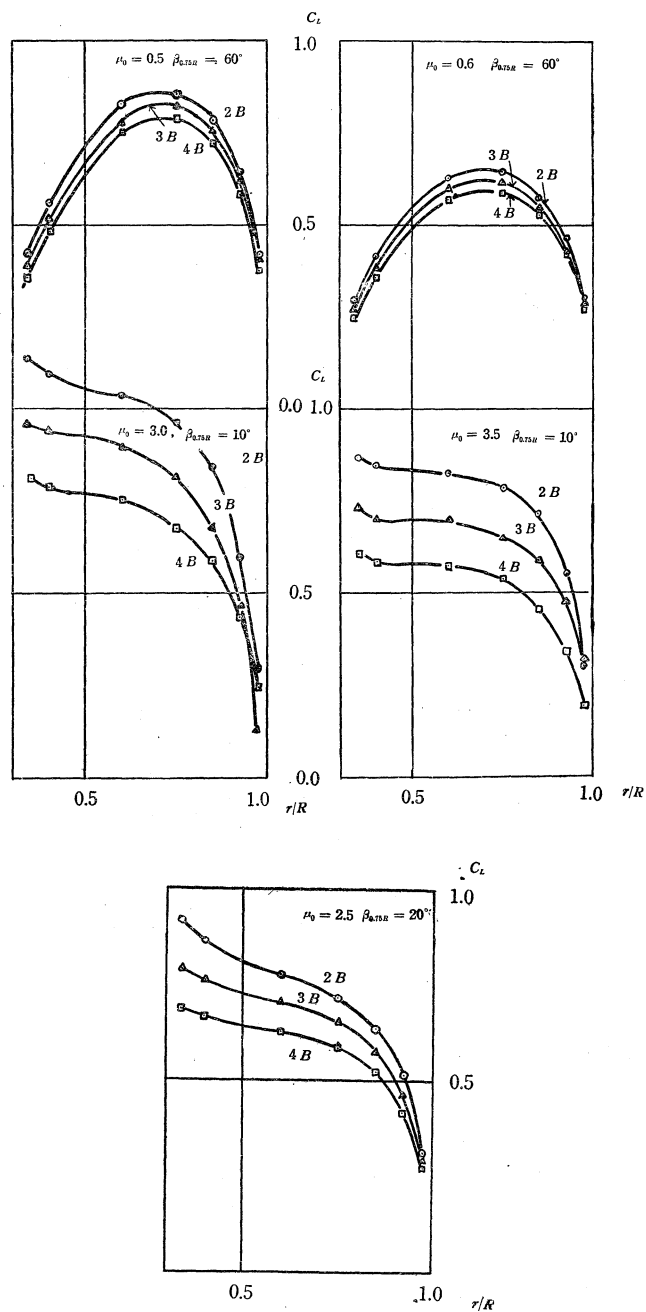


FIG. 19. The distributions of C_L along the blade. (calculated).
 $\mu_0 = \Omega R/V$.

have a finite length of 300 mm. On the other hand, the theoretical analysis of the effect of a circular cylinder is possible only in the case of the cylinder of infinite length.

So the author tried to estimate to what extent the ring of finite length shows the performance of windmills with the ring of infinite length, and in addition, to find the order of increment of performance by the ring by some theoretical analysis.

In the calculation the author used Takeyama's method combined with the author's method previously stated. Takeyama¹²⁾ solved the velocity field by helical vortices of strength I' and cylindrical circular boundary, and obtained the additional induced velocity at the blade element due to the interference of cylinder wall in the following form:

$$w_t^* = \frac{B^2 \mu_0 I}{2 \pi r} \sum_{m=1}^{\infty} \frac{m I'_{Bm}(B m \mu_0) K'_{Bm}(B m \mu') I_{Bm}(B m \mu)}{I'_{Bm}(B m \mu')}, \quad (24)$$

where

I and K : modified Bessel functions,

$$\mu' = \frac{\Omega r'}{V}$$

$$\mu_0 = \frac{\Omega r_0}{V}$$

$$\mu = \frac{\Omega r}{V}$$

r' : the inner radius of the cylinder,

r_0 : the radius of helical vortices.

Using the Nicholson's asymptotic formulas for I and K ¹³⁾ for large values of order and argument

$$I_{Bm}(B m \mu) = \left[\frac{1}{2 \pi B m \sqrt{1 + \mu^2}} \right]^{1/2} e^{Bm \{ \sqrt{1 + \mu^2} - 1/2 \log e \frac{\sqrt{1 + \mu^2} + 1}{\sqrt{1 + \mu^2} - 1} \}}$$

$$K_{Bm}(B m \mu) = \left[\frac{\pi}{2 B m \sqrt{1 + \mu^2}} \right]^{1/2} e^{-Bm \{ \sqrt{1 + \mu^2} - 1/2 \log e \frac{\sqrt{1 + \mu^2} + 1}{\sqrt{1 + \mu^2} - 1} \}},$$

Equation (23) is written as follows:

$$w_t^* = \frac{B \Gamma}{4 \pi r} \left[\frac{1 + \mu_0^2}{1 + \mu^2} \right]^{1/4} \left[\frac{1}{1 - e^{-B(t_1 + t_2)}} + \frac{1}{2 B} \left\{ \frac{1}{\mu_0} \left(1 + \frac{1}{\mu_0^2} \right)^{-3/2} \right. \right. \\ \left. \left. - \frac{2}{\mu'} \left(1 + \frac{1}{\mu'^2} \right)^{-3/2} \right\} \log e \frac{1}{1 - e^{B(t_1 + t_2)}} \right], \quad (25)$$

¹²⁾ H. Takeyama: Helical Vortices and Cylindrical Boundaries of Circular Cross Section (in Japanese), Journal of the Japan Society for Applied Mechanics, Vol. 3, No. 13, January 1950. And see the APPENDIX of the present paper.

¹³⁾ S. Kawada: *loc. cit.* p. 11.

where

$$\left. \begin{aligned} w_t^* &: \text{additional tangential induced velocity by the circular cylinder,} \\ t_1 &= f(\mu_0) - f(\mu') \\ t_2 &= f(\mu) - f(\mu') \\ f(\mu) &= \sqrt{1 + \mu^2} + \frac{1}{2} \log e \frac{\sqrt{1 + \mu^2} - 1}{\sqrt{1 + \mu^2} + 1}. \end{aligned} \right\} (26)$$

According to Kawada, the continuous distribution of circulation along a blade is replaced by constant circulations as shown in Figure 20.

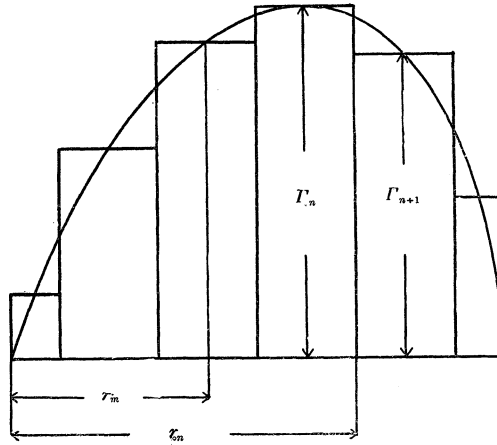


FIG 20.

(The tip vortex corresponds to Γ_N)

At every step of this discontinuous distribution of circulation there are the free vortices, for examples, at $r = r_{0n}$ the free vortex of the strength $(\Gamma_{n+1} - \Gamma_n)$. Superposing the effects of these free vortices, we obtain the equation which gives the tangential component of induced velocity at $r = r_m$ as follows:

$$\begin{aligned} \left(\frac{w_t^*}{V} \right)_{r=r_m} &= \frac{1}{4 \left(\frac{r_m}{R} \right)} \sum_{n=1}^N \left(\frac{B \Gamma_{n+1}}{\pi V R} - \frac{B \Gamma_n}{\pi V R} \right) \left[\frac{1 + \mu_{0n}^2}{1 + \mu^2} \right]^{1/4} \left[\frac{1}{1 - e^{-B(t_{1n} + t_{2m})}} \right. \\ &\quad \left. + \frac{1}{2B} \left\{ \frac{1}{\mu_{0n}} \left(1 + \frac{1}{\mu_{0n}^2} \right)^{-3/2} - \frac{2}{\mu'} \left(1 + \frac{1}{\mu'^2} \right)^{-3/2} \right\} \log e \frac{1}{1 - e^{B(t_{1n} + t_{2m})}} \right], \end{aligned} \quad (27)$$

where

$$t_{1n} = f(\mu_{0n}) - f(\mu'),$$

$$t_{2m} = f(\mu_m) - f(\mu'),$$

and

$$\Gamma_{N+1} = 0.$$

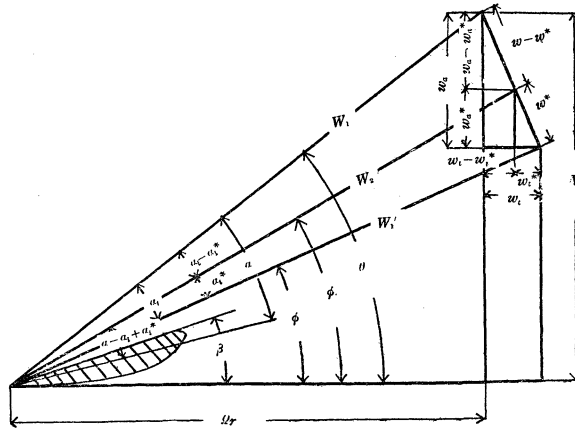


FIG. 21. The wind speed diagram for the blade element at $r = r_m$ when a circular cylinder is attached to the outside of a windmill.

This non-dimensional form of w_i^* is equal to the additional induced angle of attack α_i^* . For, when the induced angle attack is small, as seen in Figure 21, the additional induced angle of attack is written in the following form.

$$\alpha_i^* = \frac{w^*}{W_2} \div \frac{w^*}{W_1} \div \frac{w_t^* \sqrt{1 + \mu^2}}{V \sqrt{1 + \mu^2}} = \frac{w_t^*}{V}.$$

In Figure 21 $\alpha_i - \alpha_i^*$ is the resultant induced angle of attack at the blade element $r = r_m$, where α_i is the induced angle of attack of windmill alone. In order to calculate α_i , it is necessary to use the Kawada's formula¹⁴⁾, but the author uses Equation (14) for simplicity.¹⁵⁾ Substituting $\alpha_i - \alpha_i^*$ for the α_i of Equation (2), the relation between the lift coefficient C_L and the effective angle of attack $\alpha - \alpha_i + \alpha_i^*$ is given by

$$C_L = 2\pi k (\alpha - \alpha_i + \alpha_i^*) \quad (28)$$

Substituting C_L , α_i and α_i^* of Equation (17), (14) and (27) in Equation (28), we get

$$\left(\frac{B\Gamma'}{\pi V R} \right)_1 \left[\frac{1}{4} \left[\frac{1 + \mu_{01}^2}{1 + \mu_m^2} \right]^{1/4} \left[\frac{1}{1 - e^{-B(t_{11} + t_{2m})}} + \frac{1}{2B} \left\{ \frac{1}{\mu_{01}} \left(1 + \frac{1}{\mu_{01}^2} \right)^{-3/2} - \frac{2}{\mu'} \left(1 + \frac{1}{\mu'^2} \right)^{-3/2} \right\} \log e \frac{1}{1 - e^{B(t_{11} + t_{2m})}} \right] \right] \\ + \left(\frac{B\Gamma}{\pi V R} \right)_2 \left[\frac{1}{4} \left[\frac{1 + \mu_{02}^2}{1 + \mu_m^2} \right]^{1/4} \left[\frac{1}{1 - e^{-B(t_{12} + t_{2m})}} + \frac{1}{2B} \left\{ \frac{1}{\mu_{02}} \left(1 + \frac{1}{\mu_{02}^2} \right)^{-3/2} - \frac{2}{\mu'} \left(1 + \frac{1}{\mu'^2} \right)^{-3/2} \right\} \log e \frac{1}{1 - e^{B(t_{12} + t_{2m})}} \right] \right]$$

¹⁴⁾ S. Kawada: *loc. cit.*, p. 22.

¹⁵⁾ Considering the agreement of the calculated results by the author's method with Kawada's one, the use of Equation (14) will not introduce so many errors.

$$\begin{aligned}
& -\frac{1}{4} \left[\frac{1 + \mu_{01}^2}{1 + \mu_m^2} \right]^{1/4} \left[\frac{1}{1 - e^{-B(t_{11} + t_{2m})}} + \frac{1}{2B} \left\{ \frac{1}{\mu_{01}} \left(1 + \frac{1}{\mu_{01}^2} \right)^{-3/2} \right. \right. \\
& \quad \left. \left. - \frac{2}{\mu'} \left(1 + \frac{1}{\mu'^2} \right)^{-3/2} \right\} \log e \frac{1}{1 - e^{B(t_{11} + t_{2m})}} \right] + \dots \\
& + \left(\frac{BF}{\pi VR} \right)_m \left[\frac{1}{4} \left[\frac{1 + \mu_{0m}^2}{1 + \mu_m^2} \right]^{1/4} \left[\frac{1}{1 - e^{-B(t_{1m} + t_{2m})}} + \frac{1}{2B} \left\{ \frac{1}{\mu_{0m}} \left(1 + \frac{1}{\mu_{0m}^2} \right)^{-3/2} \right. \right. \right. \\
& \quad \left. \left. - \frac{2}{\mu'} \left(1 + \frac{1}{\mu'^2} \right)^{-3/2} \right\} \log e \frac{1}{1 - e^{B(t_{1m} + t_{2m})}} \right] \\
& - \frac{1}{4} \left[\frac{1 + \mu_{0m-1}^2}{1 + \mu_m^2} \right]^{1/4} \left[\frac{1}{1 - e^{-B(t_{1m-1} + t_{2m})}} + \frac{1}{2B} \left\{ \frac{1}{\mu_{0m-1}} \left(1 + \frac{1}{\mu_{0m-1}^2} \right)^{-3/2} \right. \right. \\
& \quad \left. \left. - \frac{2}{\mu'} \left(1 + \frac{1}{\mu'^2} \right)^{-3/2} \right\} \log e \frac{1}{1 - e^{B(t_{1m-1} + t_{2m})}} \right] \\
& \quad \left. + \frac{1}{4\kappa_m} + \frac{1}{2\pi k_m s_m \sqrt{1 + \mu_m^2}} \right] + \dots \\
& + \left(\frac{BF}{\pi VR} \right)_N \left[\frac{1}{4} \left[\frac{1 + \mu_{0N}^2}{1 + \mu_m^2} \right]^{1/4} \left[\frac{1}{1 - e^{-B(t_{1N} + t_{2m})}} + \frac{1}{2B} \left\{ \frac{1}{\mu_{0N}} \left(1 + \frac{1}{\mu_{0N}^2} \right)^{-3/2} \right. \right. \right. \\
& \quad \left. \left. - \frac{2}{\mu'} \left(1 + \frac{1}{\mu'^2} \right)^{-3/2} \right\} \log e \frac{1}{1 - e^{B(t_{1N} + t_{2m})}} \right] \\
& - \frac{1}{4} \left[\frac{1 + \mu_{0N-1}^2}{1 + \mu_m^2} \right]^{1/4} \left[\frac{1}{1 - e^{-B(t_{1N-1} + t_{2m})}} + \frac{1}{2B} \left\{ \frac{1}{\mu_{0N-1}} \left(1 + \frac{1}{\mu_{0N-1}^2} \right)^{-3/2} \right. \right. \\
& \quad \left. \left. - \frac{2}{\mu'} \left(1 + \frac{1}{\mu'^2} \right)^{-3/2} \right\} \log e \frac{1}{1 - e^{B(t_{1N-1} + t_{2m})}} \right] \Big] \\
& = \alpha_m \left(\frac{r_m}{R} \right) \tag{29},
\end{aligned}$$

where the suffix m means the corresponding values at $r = r_m$, and $m = 1, 2, \dots, N$.

Solving these simultaneous equations of N variables, $(BI/\pi VR)_1, (BI/\pi VR)_2, \dots, (BI/\pi VR)_N$, we get the distributions of the circulation along the blade of the windmills interfered by the circular cylinder of infinite length. If some part of radius is covered by the boss, the circulation at these parts will vanish, so that the number of equations is reduced by this number of circulations. The author calculated the performance of windmills with the circular cylinder in the following conditions:

- $B = 2$ and 3 ,
- $\beta_{0.75R} = 50^\circ$,
- $\Omega R/V = 0.8$,
- clearance between tips of windmills and the wall of cylinder
= 10 mm,¹⁶⁾
- $r' = 0.510$ m.

The data of the blade and the airfoil are shown in Table 1.

¹⁶⁾ The clearance was not determined exactly, because the circular cylinder used in our experiment was not a truly circular one and the tips of blades does not form a circular arc in this angle of blade, so that the value of 10 mm is an average value.

These conditions nearly correspond to the ones at the C_{\max} . Because $\Omega R/V$ is small, the Nicholson's asymptotic formulas may show some error, but this error is not regarded here. At the maximum power states, the windmills are heavily loaded, so that the induced velocity is considerably large. Therefore the calculations are performed up to the second approximation.

In the second approximation, the Equations (5) and (7) must be used, instead of (17) and (14) to form the simultaneous equations (29). Before substitute these Equations (5) and (7) in (28), we shall change them to the more convenient form to the calculation of the second approximation.

Now we put

$$\begin{aligned} V - w_a &= V' \\ \Omega r + w_t &= (\Omega r)' \\ \mu'' &= (\Omega r)' / V'. \end{aligned}$$

Then, as can be seen in Figure 17, we get

$$W_1' = V' \sqrt{1 + \mu''^2}. \quad (4)'$$

By (4)' and (3) the lift coefficient is expressed by

$$C_L = \left(\frac{B \Gamma}{\pi V' R} \right) \frac{1}{s \left(\frac{r}{R} \right) \sqrt{1 + \mu''^2}}, \quad (5)'$$

and from (1) and (5)' the induced angle of attack for the windmill alone is given by

$$\alpha_i = \left(\frac{B \Gamma}{\pi V' R} \right) \frac{1}{4 \kappa (r/R)}, \quad (7)'$$

where $\cos \alpha_i$ is equalized to 1 approximately. These equations correspond to Equations (5) and (7), and are the same form with Equations (17) and (14). So if we substitute the variables μ_m , μ_{0n} , μ' , V and κ which appear in Equation (29) by the values corresponding to μ'' , we can obtain the simultaneous equations by which the values of $(B\Gamma/\pi V' R)_m$ of the second or higher approximation are obtained.

The method of the determination of μ'' is as follows:

In the second approximation the pitch angles of the vortex sheets are not the ones of the uniform pitch in general, but we shall assume that the pitch of the vortex sheet to be uniform approximately, and as the representative pitch we shall take the value at 75 per cent of radius of the windmill.¹⁷⁾ Assuming the uniform pitch we can obtain the value of μ'' at radius r by

$$\mu'' = \cot \phi_1 \Big|_{r/R=0.75R} \cdot \frac{1}{0.75} \left(\frac{r}{R} \right) = \mu''_{0.75R} \frac{1}{0.75} \left(\frac{r}{R} \right).$$

In our calculation the values of ϕ_1 (see Figure 21) at $r = 0.75 R$ is about 54° in the first approximation, so that

$$\mu''_{0.75R} = \cot 54^\circ = 0.727,$$

¹⁷⁾ This idea is due to Kawada. *loc. cit.* p. 51.

and consequently we obtain

$$(\Omega R)/V' = \frac{0.727}{0.75} \doteq 0.97 \quad \text{at the tip of the blades}$$

and

$$\mu'' = 0.97 (r/R) \quad \text{at } r = r.$$

The values of μ'' are affected by the number of blades B , but we do not regard this difference.

By solving Equation (29) which corresponds to μ'' , we obtain the $(B\Gamma/\pi V'R)$ of the second approximation, and by the following formulas which can be obtained by the same simple method of calculation which is used to obtain Equation (12),

$$\left. \begin{aligned} C_w &= 2 \int_{\text{boss}}^1 \left[\left(\frac{B\Gamma}{\pi V'R} \right) \mu'' + C_D s \sqrt{1 + \mu''^2} \left(\frac{r}{R} \right) \right] \frac{1 + \mu^2}{1 + \mu''^2} d\left(\frac{r}{R} \right) \\ C_a &= 2 \int_{\text{boss}}^1 \left[\left(\frac{B\Gamma}{\pi V'R} \right) - C_D s \sqrt{1 + \mu''^2} \mu'' \left(\frac{r}{R} \right) \right] \frac{1 + \mu^2}{1 + \mu''^2} d\left(\frac{r}{R} \right) \\ C_l &= C_a \frac{\Omega R}{V} \end{aligned} \right\} (12)',$$

(where we put $\cos^2(\alpha_i - \alpha_{i*}) = 1$ approximately),

we can obtain the values of C_a , C_l and C_w for the windmills with the cylinder. In Equation (12)' μ and $\Omega R/V$ remains to be the values which are used in the first approximation throughout the calculation, that is, in this example $\mu = 0.8 (r/R)$ and $\Omega R/V = 0.8$. To increase the accuracy of the calculation the μ'' in the Equation (12)' is obtained by the following procedure.

The values of $(B\Gamma/\pi V'R)$ obtained from the last approximation are substituted in Equation (5)', and we obtain C_L . Next, from the general relation between the effective angle of attack α_e and the lift coefficient C_L

$$2\pi k \alpha_e = C_L,$$

we calculate α_e . Then, as the effective angle of attack α_e is given by (see Figure 21)

$$\alpha_e = \alpha - \alpha_i + \alpha_i^*,$$

the angle ϕ_1 is obtained from the formula

$$\phi_1 = \theta - (\alpha_i - \alpha_i^*) = \theta - (\alpha - \alpha_e).$$

Thus the μ'' which is used in Equation (12)' is given by

$$\mu'' = \cot \phi_1.$$

The results of calculation are as follows:

B	C_d	C_l	C_w	
2	0.083 (0.071)	0.066 (0.057)	0.085 (0.076)	Calcul.
	0.086 (0.069)	0.069 (0.055)	0.096 (0.086)	Exper.
3	0.114 (0.100)	0.091 (0.080)	0.120 (0.107)	Calcul.
	0.114 (0.095)	0.091 (0.076)	0.143 (0.106)	Exper.

The numbers in the brackets show the corresponding values for the windmill alone, and they are calculated by the method of paragraph 4 up to the second approximation.

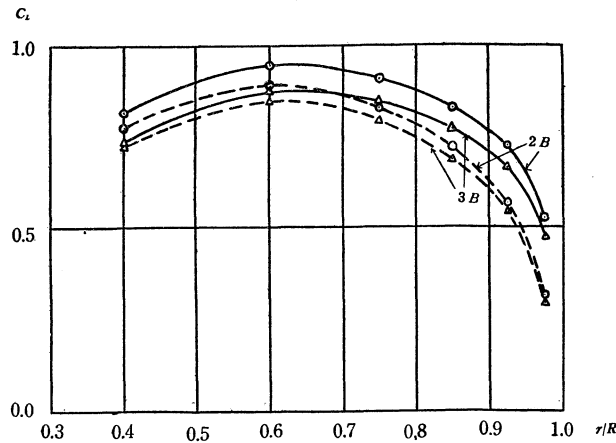


FIG. 22. The comparison of distributions of C_L along the blades in the cases when circular cylinders are attached and detached. (calculated).

—: with a cylinder.
 ----: without a cylinder.

The results of calculation does not agree so well with the experimental ones, but considering from these theoretical and experimental results, we can recognize that the cylinder of finite length has nearly the same effect with the cylinder of infinite length, and the gain in the performances due to the cylinder amounts to this order.

The calculated distribution of C_L along the blade are compared in Figure 22. We can see that by attaching the cylinder the tip losses of the windmills are reduced and the high values of C_L are maintained up to near the tips of windmills.

By the method mentioned above, we can also calculate the performance of the windmill alone. The equation by which $(B\Gamma/\pi V'R)$ of the second or higher approximation is calculated is given, from Equations (2), (5)' and (7)', by

$$\left(\frac{B\Gamma}{\pi V'R}\right) = \frac{\alpha(r/R)}{\frac{1}{4\kappa} + \frac{1}{2k\pi\sqrt{1+\mu'^2}}} \quad (9)',$$

where κ is obtained by r/R , $\sin \phi = 1/\sqrt{1 + \mu'^2}$, and Figures 17 (a), (b) and (c).

This equation is the same form with (13).

ϕ and α_e are obtained, as before, by

$$\phi = \tan^{-1} \mu - \alpha_i \quad (10)$$

$$\alpha_e = \alpha - \alpha_i. \quad (11)$$

The first approximation is performed by using Equations (13), (14), (15), (16) and (17), and Equations (9)', (7)', (10), (11), (5)', and (12)' are used in the second or higher approximations. This method of the calculation of the performance of the windmill alone would be rather simpler than the one shown in Paragraph 4.

6. The estimation of the effect of the fuselage on the performance of the windmill. In the present experiments the boss parts of windmills are covered with the cylinder of radius 0.135 m (see Figure 1). So it is necessary to estimate the amount of the interference of the fuselage in the C_a , C_l and C_w . The author tried to find this effect by calculation using the method of Takeyama¹⁸⁾ combined with the author's one. By him, when there is the single helical vortices of strength Γ at $r=r_0$, the additional tangential induced velocity w_t^* which is caused by the existence of the circular cylinder or the fuselage in the inner region of the helical vortices is given by

$$w_t^* = \frac{B\Gamma}{4\pi r} \left[1 + \left[\frac{1 + \mu_0^2}{1 + \mu^2} \right]^{1/4} \left[\frac{1}{e^{B(t_1+t_2)} - 1} + \frac{1}{2B} \left\{ \frac{1}{\mu_0} \left(1 + \frac{1}{\mu_0^2} \right)^{-3/2} - \frac{2}{\mu'} \left(1 + \frac{1}{\mu'^2} \right)^{-3/2} \right\} \log e \frac{1}{1 - e^{-B(t_1+t_2)}}} \right] \right], \quad (25)'$$

where

$$\left. \begin{aligned} t_1 &= f(\mu_0) - f(\mu') \\ t_2 &= f(\mu) - f(\mu') \\ f(\mu) &= \sqrt{1 + \mu^2} + \frac{1}{2} \log e \frac{\sqrt{1 + \mu^2} - 1}{\sqrt{1 + \mu^2} + 1} \\ &\text{and } r' \text{ is the radius of the fuselage,} \\ &\text{and } \mu' = \Omega r' / V. \end{aligned} \right\} \quad (26)'$$

As mentioned in Paragraph 5, in the practical case we assume that there is the vortex of the strength $\Gamma_{n+1} - \Gamma_n$ at $r=r_{0n}$, and then the additional induced velocity at $r=r_m$ is given by

$$\left(\frac{w_t^*}{V} \right)_{(r/R)=(r_m/R)} = \frac{1}{4(r_m/R)} \sum_{n=1}^N \left(\frac{B\Gamma_{n+1}}{\pi VR} - \frac{B\Gamma_n}{\pi VR} \right) \left[1 + \left[\frac{1 + \mu_{0n}^2}{1 + \mu_m^2} \right]^{1/4} \left[\frac{1}{e^{B(t_{1n}+t_{2m})} - 1} + \frac{1}{2B} \left\{ \frac{1}{\mu_{0n}} \left(1 + \frac{1}{\mu_{0n}^2} \right)^{-3/2} - \frac{1}{\mu'} \left(1 + \frac{1}{\mu'^2} \right)^{-3/2} \right\} \log e \frac{1}{1 - e^{-B(t_{1n}+t_{2m})}} \right] \right], \quad (27)'$$

¹⁸⁾ Takeyama: *loc. cit.*

where $t_{1n} = f(\mu_{0n}) - f(\mu'),$

$$t_{2m} = f(\mu_m) - f(\mu'),$$

and $\Gamma_{\Lambda+1} = 0.$

This value of (w_i^*/V) is substitute for the α_i^* in the equation

$$C_L = 2\pi k(\alpha - \alpha + \alpha^*) \quad (28)$$

and the same form of a system of simultaneous equations of N variables $(BF/\pi VR)_1, (BF/\pi VR)_2, \dots, (BF/\pi VR)_N,$ is obtained. The calculations which follows after the solution of these equations are the same with Paragraph 5.

The results of the calculation are as follows:

C_d	C_l	C_w	
0.071	0.057	0.075	windmill alone (calcu.)
0.073	0.058	0.077	with fuselage (calcu.)
0.069	0.055	0.086	(experi.)

the conditions for the calculation:

$$B = 2$$

$$\Omega R/V = 0.8$$

$$r'/R = 0.27$$

$$\beta_{0.75R} = 50^\circ.$$

The conditions correspond to the case in which B and $\Omega R/V$ are small, so that the effect of the fuselage is large. But, as can be seen in the table, even in these conditions, the effect of fuselage is not so much, so that we may conclude that the present results of the experiment shows almost the pure performances of the windmills alone, and the little difference between the results of the theory and the experiments, which can be seen in Table 5, can be attribute to the effect of fuselage to some extent.

7. Conclusions.

(1) The C_d , C_l and C_w curves are obtained for 2, 3, 4 and 6 bladed windmills.

(2) There is some limits to increase the power by means of reducing the angle of blades, and the angle corresponding to this limiting condition, in the author's experiment, is about 10° for 2 and 3 bladed windmills, and for 4 and 6 bladed windmills it is near the angle of 20° .

(3) For the fast running windmills the increase of the number of blades does not result in the increase in the power of windmills, even if the number of blades increases beyond three.

(4) If the strong starting torque is not required, the best windmill is the three bladed windmill.

(5) The distributions of C_L along the blade are calculated for two, three and four bladed windmills at near the state of maximum power.

(6) The C_L of blade elements of windmills used in the author's experiment is below 1 at the working conditions near the maximum power, and

the values of C_z become smaller as the number of blades increases. This trend is remarkable at the fast running windmills.

(7) The performances of the windmills with a ring are made clear by the experiments and the theoretical analysis.

(8) The gain of the power of windmills by attaching a ring is at most 30 per cent, and we find that the increase in power shown in the Sanuki's paper is mainly due to the acceleration of wind velocity by the ventilator tube.

The author wishes to acknowledge the assistance rendered in this investigation through a grant in aid for fundamental scientific research from the Ministry of Education in Japan.

The author should like to express his sincere thankfulness to Prof. Y. Watanabe for his kind encouragement and valuable suggestions through these researches.

Asst. Ôhira and Noda, and Empl. Sada assisted the author's work and Mr. Moribe and Mr. Yamada made the apparatuses and models. The author is very thankful to them.

APPENDIX

Takeyama's solution

The velocity potential in the velocity field induced by the helical vortices which exist for behind the windmills or propellers is given by Kawada as the solution of the differential equation

$$\frac{\partial^2 \phi}{\partial \mu^2} + \frac{1}{\mu} \frac{\partial \phi}{\partial \mu} + \left(1 + \frac{1}{\mu^2}\right) \frac{\partial^2 \phi}{\partial \zeta^2} = 0,$$

where
$$\mu = \frac{\Omega r}{V} \quad \text{and} \quad \zeta = \theta - \frac{\Omega z}{V},$$

z is measured along the center line of the helical vortices, and r, θ are the polar coordinates in the plane perpendicular to z axis.

The solutions of the equation for the equally spaced B helical vortices are

$$\phi_0 = -\frac{B\mu_0 \Gamma}{\pi} \sum_{m=1}^{\infty} I'_{Bm}(Bm\mu_0) K_{Bm}(Bm\mu) \sin Bm\zeta \quad \text{for } \mu \geq \mu',$$

$$\phi_i = -\frac{B\Gamma}{2\pi} \left(\frac{B}{\pi} - \zeta\right) - \frac{B\mu' \Gamma}{\pi} \sum_{m=1}^{\infty} K'_{Bm}(Bm\mu_0) I_{Bm}(Bm\mu) \sin Bm\zeta$$

for $\mu \leq \mu'$.

When the field is bounded by the circular cylinder situated at the outside of the vortices, the radial component of the induced velocity must be zero, so that the potential ϕ_0 for this velocity field must satisfy the condition,

$$\frac{\partial \phi_0}{\partial \mu} = 0 \quad \text{at } \mu = \mu'.$$

If we consider that ϕ_0 is corrected by ϕ^* through the cylinder, we can write as $\phi_0 = \phi_0 + \phi^*$, so that the condition becomes

$$\frac{\partial \phi_0}{\partial \mu} = -\frac{\partial \phi^*}{\partial \mu} \quad \text{at } \mu = \mu'.$$

In addition to this the condition $\phi^* \rightarrow 0$ as $\mu \rightarrow 0$ is necessary.

The solution which satisfy these conditions is

$$\phi^* = \frac{B\mu_0 \Gamma}{\pi} \sum_{m=1}^{\infty} \frac{I'_{Bm}(Bm\mu_0) K'_{Bm}(Bm\mu') I_{Bm}(Bm\mu)}{I'_{Bm}(Bm\mu')} \sin Bm\zeta,$$

and the additional tangential induced velocity at the blade elements of the windmills or the propellers is given by

$$w_t^* = \frac{B^2 \mu_0 \Gamma}{2\pi r} \sum_{m=1}^{\infty} m \frac{I'_{Bm}(Bm\mu_0) K'_{Bm}(Bm\mu') I_{Bm}(Bm\mu)}{I'_{Bm}(Bm\mu')}.$$

(Received April 27, 1953)